A Mathematical Exploration of Strategies to Combat and Control the Zika Virus

A Thesis
Presented to
The Mathematics and Computer Science Department
Colorado College
In Partial Fulfillment of the Requirements for the Degree
Bachelor of Arts

Lauren Stierman
Faculty Advisor: Dr. Andrea Bruder

March 2020

A Mathematical Exploration of Strategies to Combat and Control the Zika Virus

Lauren Stierman
Faculty Advisor: Dr. Andrea Bruder

Abstract

The Zika Virus (ZIKV) – transmitted both vectorially by mosquitoes and sexually among humans – causes short-term and non-lethal infections but also induces acute complications during pregnancy, such as microcephaly. In this paper, we employ an epidemiological model of both modes of transmission in order to assess key strategic efforts to prevent the spread of infection. We consider self-protection from mosquito bites, depletion of mosquito populations, and control of sexual transmission; evaluating their respective effects on the spread of Zika Virus infections. We also propose two extensions of this model which incorporate live and passive vaccination. Using these models, we investigate the influence of such immunization strategies, specifically examining the significance of vaccination in relation to the time at which an outbreak commences. For each strategy, we evaluate its practicality and its capacity to limit or decelerate transmission of ZIKV.

1 Introduction to Zika Virus

1.1 Global Impact

Declared as a Public Health Emergency of International Concern (PHEIC) by the World Health Organization (WHO) on February 1st, 2016 [7], the spread of the Zika virus (ZIKV) constitutes a global health challenge which has affected a sum of 86 countries or territories across the Americas, the Pacific, Asia, and Africa [19]. While no longer an emergent affair, the spread of ZIKV maintained its status as an international crisis for over ten months in 2016 following the intense 2015 outbreak [20]. See Figure 1 [17] for a list of the 68 areas which were impacted by ZIKV between 2007 and August 3, 2016, 65 of which recorded ZIKV cases between 2015 and 2016. This list is categorized by the specific level of impact on each country or territory by the 2015-2016 outbreak. The potential for a similar Zika crisis illuminates the need for surveillance of the disease and global preparedness for responding to it [16, 20]. Currently, ZIKV levels remain low, but the virus is still spreading [16]; thus, it is a crucial time to strategize how to best maintain these low levels and prevent another epidemic [16, 20].

Classification	WHO Regional Office	Country / territory / area	Total
Category 1: Countries with a first reported outbreak from 2015 onwards	AFRO	Cabo Verde; Guinea-Bissau	2
	AMRO/PAHO	Anguilla; Antigua and Barbuda; Argentina; Aruba; Barbados; Belize; Bolivia (Plurinational State of), BONAIRE, SINT EUSTATIUS and SABA – Netherlands*; Brazil; Colombia; Costa Rica; Cuba; Curaçao; Dominica; Dominican Republic; Ecuador; El Salvador; French Guiana; Grenada; Guadeloupe; Guatemala; Guyana; Haiti; Honduras; Jamaica; Martinique; Mexico; Nicaragua; Panama; Paraguay; Peru; Puerto Rico; Saint Barthélemy; Saint Lucia; Saint Martin; Saint Vincent and the Grenadines; Sint Maarten; Suriname; Trinidad and Tobago; Turks and Caicos; United States of America; United States Virgin Islands; Venezuela (Bolivarian Republic of)	43
	WPRO	American Samoa; Fiji; Marshall Islands; Micronesia (Federated States of); Samoa; Tonga	6
Subtotal			51
Category 2: Countries with possible endemic transmission or evidence of local mosquito-borne Zika infections in 2016	SEARO	Indonesia; Thailand	2
	WPRO	Philippines; Viet Nam	2
Subtotal			4
Category 3: Countries with evidence of local mosquito-borne Zika infections in or before 2015, but without documentation of cases in 2016, or outbreak terminated	AFRO	Gabon	1
	PAHO/AMRO	ISLA DE PASCUA – Chile**	1
	SEARO	Bangladesh; Maldives	2
	WPRO	Cambodia; Cook Islands**; French Polynesia**; Lao People's Democratic Republic; Malaysia; New Caledonia; Papua New Guinea; Solomon Islands; Vanuatu	9
Subtotal			13
Total			68

*This includes confirmed Zika virus cases reported in BONAIRE – Netherlands, SINT EUSTATIUS and SABA – Netherlands.
**These countries and territories have not reported Zika virus cases in 2015 or 2016.

Figure 1: Countries and Territories with Vectorial ZIKV Transmission, Affected by the 2015-2016 Epidemic

1.2 Transmission

ZIKV is a flavivirus principally transmitted in the tropics and subtropics by Aedes mosquitos – primarily Aedes aegypti – which bite during the daytime and are also responsible for the transmission of chikungunya, dengue, Japanese encephalitis, and yellow fever [7, 19]. Such vectorial transmission occurs horizontally both from infectious *vectors* – the mosquitoes which carry the virus – to healthy humans and from infectious humans to healthy vectors, all through mosquito bites [7, 13]. An infection with ZIKV causes mild fever, rash, conjunctivitis, muscular and joint pain (arthralgia), headache, and malaise – symptoms similar to influenza [8] – generally for a span of 2-7 days [7, 19]. While not normally lethal [7], infection is most serious when occurring during pregnancy, as ZIKV can spread vertically from mother to fetus and lead to *microcephaly* – a condition causing an abnormally small head, deriving from irregular brain development or the depletion of brain tissue – as well as other congenital complications in the baby such as limb contractures, abnormal muscle tone, hearing difficulties, and eye malformations [13, 19]. Approximately 1 in 5 infections with ZIKV are symptomatic [7], yet both symptomatic and asymptomatic infections can be associated with congenital complications in infants [19]. Additionally, ZIKV has been linked to preterm birth, miscarriage, and stillbirth, as well as Guillain-Barré syndrome, neuropathy, and myelitis [19].

ZIKV was first identified in monkeys in Uganda in 1947 in the Zika forest, and infection had spread to humans in Uganda and Tanzania by 1952 [7, 19]. However, infection in humans remained rare from the 1960s-1980s, with the first outbreak on the Island of Yap in the North Pacific in April 2007 [7, 19]. Continuing to spread, the virus was linked to microcephaly in Brazil in October of 2015 [7, 19], four months before the WHO categorized its spread as an international health emergency. See Figures 2 – 4 [9] for a topographical display of the timeline of the spread of ZIKV.

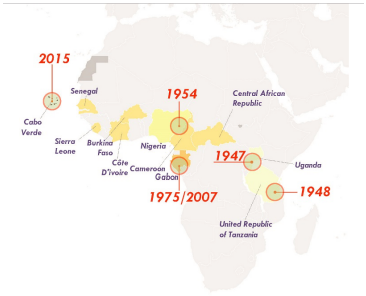

Figure 2: Geographical timeline of the spread of ZIKV in Africa

Figure 3: Geographical timeline of the spread of ZIKV in Asia and the Pacific

Figure 4: Geographical timeline of the spread of ZIKV in the Americas

In addition to transmission among mosquitoes to humans and transmission from mother to child, ZIKV can be transmitted horizontally from human to human through heterosexual sexual contact, blood transfusion, and organ transplant [7, 13, 19]. However, the dynamics of sexual transmission of ZIKV are not well-understood, and this type of transmission is estimated to account for only 4.437% of Zika infections,

with a 95% confidence interval [7]. But regardless of this small percentage, this additional mode of transmission can heighten the severity of an epidemic, extend its duration, and disrupt efforts to contain ZIKV; while sexual transmission cannot alone institute or maintain an outbreak, it can play a key role in supporting it [7].

1.3 Response

In order to manage the spread of ZIKV, there are three main strategies: vaccination, protection from mosquito bites, and reduction of the number of mosquitoes. These strategies to avoid contracting an infection are incredibly important, as there is no specific treatment available for an infection with ZIKV – once one becomes infected, common cold and flu treatments such as rest, fluids, and over-the-counter medications are recommended. It is most important for young children, pregnant women, and women of reproductive age to protect themselves from ZIKV [19]. The first strategy, vaccination, is currently unavailable, as the creation of a vaccine is still in progress, with several types of vaccines in development, specifically by the National Institute of Allergy and Infectious Diseases (NIAID) [18, 19]. Until such a vaccine becomes available, preventative strategies are key. Mosquito bite protection includes wearing protective layers covering much of the body, using insect repellent, and covering oneself with mosquito nets while sleeping. Bite prevention through controlling mosquito populations includes eliminating or reducing mosquito breeding sites – which are marked by water collection – and utilizing larvicides and insecticides [7, 19]. Additional strategies to control transmission of ZIKV among humans include measures to increase availability to contraception, limit unprotected sex, and provide women access to information so that they may make informed decisions about whether to become pregnant [7, 13, 19].

In response to ZIKV, the WHO has put forth the Zika Strategic Response Framework [19], which includes a number of measures to combat the virus. This is an all-inclusive framework, addressing every stage of an infection. This framework supports research efforts in prevention of ZIKV and efforts to reduce global mosquito populations, aims to advance surveillance systems for infections and their complications and to strengthen global testing facilities, and supports children and families who are impacted by ZIKV.

2 Compartmental Models

2.1 SIR modeling

2.1.1 Compartments

To construct a mathematical representation of the transmission of an infectious disease such as ZIKV, epidemiologists utilize compartmental models to demonstrate the dynamics of an epidemic. Compartmental models divide the entire population into classes and illustrate how members of the population flow from one class to the next, characterizing rates of passage between classes. A basic model [3], originally developed by W.O. Kermack and A.G. McKendrick in 1927, classifies the population into three compartments: individuals who are susceptible to infection (S), individuals who have been infected and are infective to the susceptible population (I), and removed individuals who have previously developed the disease but cannot be re-infected and can no longer infect others (R). Those in the R class may be recovered from infection with permanent immunity or physically removed from the remainder of the population through isolation or death. In this model, N expresses the size of the entire population, so $N = S + I + R$.

These three categories of individuals comprise the simple SIR model (Susceptible-Infected-Removed), characterized by a single possible path for individuals from S to I to R. Figure 5 [3] demonstrates this path.

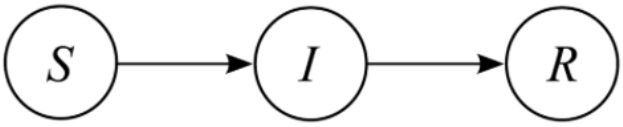

Figure 5: Flow Diagram for Basic SIR Model

In this system, the independent variable is the time t at which an outbreak begins, and flow rates between classes are represented as derivatives of the magnitude of each individual class, with respect to time. Thus, each compartment has a corresponding differential equation that expresses the number of members of the population who belong to that compartment at t, and the set of differential equations $\{S'(t), I'(t), R'(t)\}$ constitutes the model's behavior. So, the model must assume that the size of each class of individuals is a function of t that is differentiable. The model also assumes that the progression of an outbreak is *deterministic* – that the population dynamics within the system are dictated solely by their past behavior and by the model's defining features [3].

2.1.2 Model Assumptions

In order to simplify transmission dynamics, SIR modeling assumes that epidemics occur within uncomplicated systems. In addition to differentiability, determinism, and the assumptions that recovery corresponds to permanent immunity to the disease and that every member of a certain class is equally healthy or ill [4], this type of model makes the following four assumptions:

(a) Any individual has adequate interactions to spread the disease with βN other individuals per unit time, where β is the transmission rate [3]. Thus the contact rate between infective and susceptible individuals is assumed to be equivalent for every individual in these populations, and the transmission rate is assumed to be directly proportional to this contact rate [4].

(b) Individuals with infections depart from the I compartment at a rate of αI per unit time, where α is the recovery rate [3].

(c) The total population size, N, is a fixed value. Because the timeline of an epidemic is much more condensed than that of human births and deaths, we ignore any changes to N due to the natural human life cycle [3]. Thus the populations in this model are without *vital dynamics* – the regular birth and death rates in a disease-free state [4].

(d) The disease is not lethal, so N remains constant [3].

2.1.3 Differential Equations

The set of differential equations [3] is as follows:

$S' = -\beta SI$

$I' = \beta SI - \alpha I$

$R' = \alpha I$,

with initial conditions defined as $S(0) = S_0, I(0) = I_0$, and $S(0) + I(0) = N$.

So SI is an interaction term between susceptible individuals and infected individuals; this is the contact that transmits the disease at a rate of β. As transmission persists, βSI individuals depart from the S compartment and enter the I compartment. In the I compartment, as individuals recover at a rate of α, αI members leave the I compartment and enter the R compartment.

2.2 Basic Reproduction Number

Within a compartmental epidemiological model, we may quantify the severity of disease transmission using a chief comparative measure known as the *basic reproduction number* $\mathcal{R}_0$ [3, 7], which calculates the threshold for characterizing an outbreak as an *epidemic*. $\mathcal{R}_0$ denotes the number of susceptibles who become infected by a single contagious individual exposed to an entirely susceptible community, where

$\mathcal{R}_0 = \frac{\beta S_0}{\alpha}$,

assuming the initial source of the outbreak is from outside of the N individuals in the population, perhaps from a visitor to the community. Therefore $N = S_0$.

However, if the outbreak derives from within the population, perhaps from members of the community arriving home after contracting the disease abroad, then $N \approx S_0$ and $\mathcal{R}_0 = \frac{\beta N}{\alpha}$. We consider this special case.

From the definition, it follows that the larger the value of $\mathcal{R}_0$, the more critical the outbreak will be. The

threshold is set at 1 according to the following inequalities [3]:

if $\mathscr{R}_0 < 1$, disease transmission is minimal and there is no epidemic; however,

if $\mathscr{R}_0 > 1$, the disease spreads actively and we can confirm the existence of an epidemic.

For example, we consider a human population N of 100, in which a group of 25 individuals becomes exposed to and infected with a disease while travelling abroad. Upon returning to their community, with $S_0 = 75$ and $I_0 = 25$, infections spread throughout the population as follows:

Case 1: Outbreak does not constitute epidemic

With $\beta = .0005$ and $\alpha = .08$, $\mathscr{R}_0 = \frac{.0005N}{.08} = .625 < 1$. Thus each infection causes approximately .625 additional infections, and no epidemic exists. Figure 6 demonstrates that the susceptible population diminishes slightly, but transmission of the disease remains controllable. The size of the infected population reduces as time goes on, and the disease does not impact the entire population.

Case 2: Outbreak constitutes epidemic

With $\beta = .03$ and $\alpha = .08$, $\mathscr{R}_0 = \frac{.03N}{.08} = 37.5 > 1$. Thus each infection causes approximately 37.5 additional infections, and an epidemic exists. Figure 7 demonstrates that the susceptible population shrinks to 0 rapidly, and the size of the infected population spikes immediately as disease erupts throughout the community. At $t = 2$, all members of the population have been affected by the disease. Hence, conditions are much more critical than in Case 1.

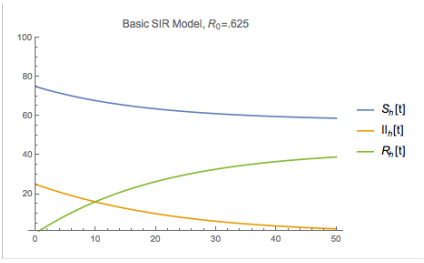

Figure 6: SIR Model with Basic Reproduction Number $\mathscr{R}_0 < 1$, Non-epidemic conditions

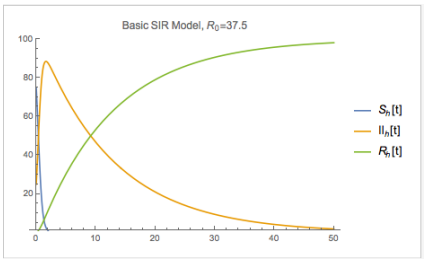

Figure 7: SIR Model with Basic Reproduction Number $\mathscr{R}_0 > 1$, Epidemic conditions

Note: All of the numerical simulations in this paper were run in Mathematica, with time plotted against the number of individuals.

2.3 More Complex Modeling

Such an SIR model is most common for viral infections such as ZIKV, while bacterial infections often utilize an SIS model (Susceptible-Infected-Susceptible) [3]. Recovery from an illness caused by bacteria normally does not protect against re-infection; hence, individuals who are no longer infected re-enter the susceptible compartment. These basic model types can be extended to account for the dynamics of more complex systems [3], such as an $SIRS$ type in which individuals enter a removed compartment following infection but are only immune to the sickness for a short period and eventually move back to the susceptible compartment. Models often have an exposed compartment (E) for individuals who have been exposed to the illness but have not yet become infective or have not yet shown symptoms, leading to $SEIR$ or $SEIS$ model types. Other common compartments include treatment compartments, vaccinated compartments, asymptomatic infection compartments, and quarantined and isolated compartments for new illnesses without vaccines in which physical distance from the susceptible population may be the only feasible method of managing disease transmission.

3 Literature Review

Since ZIKV broke out on the large scale in $2016 - 2017$, several epidemiological studies have been conducted in order to determine how to best control an outbreak of the disease. In May 2016, the model built in [11] was published as a compartmental $SEIR$ model which holds the size of the human population constant and allows for humans to transmit ZIKV back to vectors while belonging to the pre-symptomatic exposed

population. This model examines the French Polynesian ZIKV outbreak of $2013-2014$, and results indicate that ZIKV could demonstrate similar transmission dynamics to dengue virus (DENV) and that epidemic conditions in a certain location may prevent an outbreak from occurring in the same place for many years. This model only accounts for paths of ZIKV infection between mosquitoes and humans, but as time passed, more and more evidence for human-to-human transmission of ZIKV accumulated.

Published in May 2011, the study in [5] recorded a case of probable sexual transmission of ZIKV – noting that the spread of an arbovirus through sexual contact had never been recorded before. Then, the Emerging Infectious Diseases journal reported the biological presence of ZIKV in urine after reverse transcription PCR (RT-PCR) testing – published in January 2015 [8]. By February 2016, Centers for Disease Control and Prevention (CDC) had published instructions for avoiding the spread of ZIKV through sex [6]. Further, in March 2016, another report documented multiple confirmed cases of sexual transmission of ZIKV within the United States, concluding that human-to-human infections are more frequent than formerly known [6]. Reaffirming this result, the Emerging Infectious Diseases journal reported that real-time reverse transcription PCR (rRT-PCR) testing had confirmed the biological presence of ZIKV in semen – published in May 2016 [1]. In the following month, the model in [7] was published, extending the vectorial model in [11] to incorporate the impact of sexual transmission on ZIKV outbreaks. In 2017, the Applied Mathematics journal published the model in [13], which accounts for both sexual transmission of ZIKV and congenital vertical transmission from mother to fetus, as well as vectorial spread. This model considers the impacts of the use of insecticides, mosquito bite prevention, protected sexual contact, and treatment to alleviate symptoms [13].

Mathematical models which evaluate the influence of immunization strategies have also been created for ZIKV. In October 2017, the Journal of Applied Mathematics and Physics published a model [14] which employs a combination of immunization and treatment strategies to respond to ZIKV. This model assumes that when susceptible humans receive the ZIKV vaccine, they immediately become immune and are removed from the population, but their immunity is not permanent – they can re-enter the susceptible population after a certain amount of time. Results from this study indicate that while a single strategy of either vaccination or treatment can demonstrate success in mitigating transmission of ZIKV, their joint effect is more powerful[14]. Another study, published in May 2019 by Epidemiology & Infection, proposed a complex model [12] comprised of 13 differential equations, intending to measure the optimal start time for an immunization campaign to control the spread of ZIKV. This model, too, assumes that the vaccine is effective immediately, but individuals may only depart from the vaccinated compartment through natural death. Results of this study suggest that an ideal vaccination strategy will begin when the ratio of Aedes mosquitoes to humans is $1.5:1$, corresponding to the time at which the reproduction number surpasses 1. If the institution of such an immunization campaign must be delayed, this study recommends to wait no longer than the recognition of the first case of infection in the population [12].

Now, we add to this body of existing literature our mathematical analysis of the effectiveness of key strategies for responding to ZIKV. In order to evaluate such strategies, we implement a pre-existing epidemiological model of both vectorial and sexual spread of the disease, and we introduce 2 extended models which assess the impact of vaccination on population dynamics during a ZIKV outbreak – one model which confers immediate immunity to individuals who receive the vaccine, like the models in [12] and [14], and another model which includes a phase of vaccine ineffectiveness and requires individuals to pass through a susceptible vaccinated compartment before proceeding to the immune compartment.

4 A Model of Both Vectorial and Sexual Transmission of ZIKV

We consider the deterministic model of the spread of ZIKV proposed in [7]. We recall that this representation of transmission dynamics expands on the vectorial model in [11], integrating the influence of sexual transmission into the model. The time t is measured in days.

4.1 Model Assumptions

Several assumptions inform the model in [7]. Importantly, infected humans are completely immune to ZIKV following recovery. Once removed from the susceptible population, humans who will develop symptomatic infections are contagious to both humans and mosquitoes during the incubation phase. Once symptoms have developed, humans have a greater probability of infecting mosquitoes than exposed humans. Once

symptoms have ceased to appear, the viremic period concludes as humans enter the convalescent phase, in which humans are still contagious to other humans – at a lesser likelihood of transmission – yet are no longer contagious to mosquitoes, as it is assumed that ZIKV remains present in urine and semen longer than it remains in serum. However, humans who develop asymptomatic infections are neither contagious to other humans nor mosquitoes.

As the lifespan of a ZIKV outbreak is extremely short in relation to human life, the human population is assumed to be constant throughout an epidemic. It is also assumed that men and women are essentially dependent on the same epidemiological factors, and that the human sexual ratio is 1:1.

4.2 Basic Reproduction Number

For the model in [7], the basic reproduction number for ZIKV – accounting for both vectorial and sexual modes of transmission – was adjusted to fit specific data from ZIKV outbreaks in Colombia, El Salvador, and Brazil, and was computed as:

$\mathscr{R}_0 = \frac{\mathscr{R}_{hh}+\sqrt{\mathscr{R}_{hh}^2+4\mathscr{R}_{2_{hv}}}}{2}$,

where $\mathscr{R}_{hh}$ denotes the basic reproduction number for transmission among humans and $\mathscr{R}_{hv}$ denotes the basic reproduction number for transmission between humans and mosquitoes. $\mathscr{R}_0$ is calculated at 2.055 [7] with a 95% confidence interval, with only 3.044% of $\mathscr{R}_0$ represented by human-to-human transmission, also with a 95% confidence interval. Specifically, $\mathscr{R}_{hv} = 1.960$ and $\mathscr{R}_{hh} = 0.136$.

Therefore, while contagious, every human who develops a symptomatic ZIKV infection communicates the disease to approximately 2 other susceptible individuals.

4.3 Compartments

The model in [7] includes 9 compartments, 6 for humans and 3 for mosquitoes.

4.3.1 Human Population

We set N_h, the total number of humans in the population, to $20,000$ people.
We let $N_h = S_h(t) + E_h(t) + I_{h1}(t) + I_{h2}(t) + A_h(t) + R_h(t)$, where
$S_h(t)$ represents the susceptible human population at time t,
$E_h(t)$ represents the exposed human population at time t,
$I_{h1}(t)$ represents the symptomatically infected human population at time t,
$I_{h2}(t)$ represents the convalescent human population at time t,
$A_h(t)$ represents the asymptomatically infected human population at time t, and
$R_h(t)$ represents the recovered human population at time t.

4.3.2 Mosquito Population

We then set N_v, the total number of mosquitoes in the population, to $N_h * m$, where m is the average ratio of mosquitoes to humans (number of mosquitoes per human). In this system, m is initially estimated at 5, so $N_v = 100,000$.

We let $N_v = S_v(t) + E_v(t) + I_v(t)$, where
$S_v(t)$ represents the susceptible mosquito population at time t,
$E_v(t)$ represents the exposed mosquito population at time t, and
$I_v(t)$ represents the infectious mosquito population at time t.

4.4 Parameters for the Model

4.4.1 Set of Parameters

This system of equations in the model in [7] depends on the following set of parameters: $\{a, b, c, \eta, \beta, \kappa, \tau, \theta, \nu_h, \nu_v, \lambda_{h1}, \lambda_{h2}, \lambda_h, \mu_v\}$. Each parameter is defined below.

a: Mosquito biting rate, i.e. the number of times each mosquito bites each day

b: Transmission probability from an infectious mosquito to a susceptible human per bite
c: Transmission probability from a symptomatically infected human to a susceptible mosquito per bite
η: Relative human-to-mosquito transmission probability of exposed humans to susceptible mosquitoes
β: Transmission rate from symptomatically infected humans to susceptible humans, per day
κ: Relative human-to-human transmissibility of exposed humans to susceptible humans
τ: Relative human-to-human transmissibility of convalescent humans to susceptible humans
θ: Proportion of symptomatic infections, expressed as a percentage
ν_h: Intrinsic incubation rate in humans, measured in $\frac{1}{days}$
ν_v: Extrinsic incubation rate in mosquitoes, measured in $\frac{1}{days}$
λ_{h1}: Rate of acute phase, measured in $\frac{1}{days}$
λ_{h2}: Rate of convalescent phase, measured in $\frac{1}{days}$
λ_h: Rate of asymptomatic infection, measured in $\frac{1}{days}$ and
μ_v: Rate of mosquito lifespan, measured in $\frac{1}{days}$.

4.4.2 Parameter Estimation

Parameter estimates for the model in [7] derive from current known factors regarding ZIKV transmission. The Zika virus is comparable to the dengue virus, as the two viruses are arboviruses of Aedes mosquitos and cause similar infections – with related symptoms, levels of contagion, and length of incubation. Zika and dengue viruses, too, both demonstrate a high ratio of asymptomatic to symptomatic infections. Thus, some parameters for ZIKV transmission in this model are estimated from known parameters for dengue transmission. Additionally, some parameters are estimated from sexual frequency rates and knowledge of other sexually transmitted infections.

4.4.3 Flow Diagram

Figure 8 demonstrates the interplay of these parameters and the compartments of the model, where green nodes indicate non-infectious populations and red nodes indicate infectious populations. Blue arrows demonstrate possible paths for an individual human or mosquito as ZIKV progresses, black dashed arrows demonstrate avenues of human-to-human infection, and red dashed-dotted lines demonstrate avenues of mosquito-to-human and human-to-mosquito transmission.

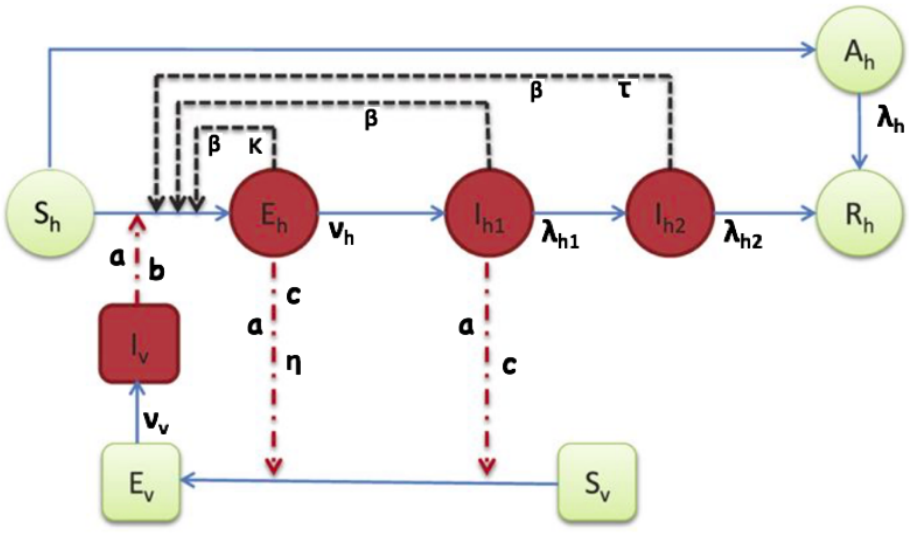

Figure 8: Flow Diagram for Transmission of ZIKV, with Both Vectorial and Sexual Modes

4.5 Differential Equations

The model in [7] comprises 9 ordinary differential equations, 6 describing the population dynamics of humans and 3 describing the population dynamics of mosquitoes. A differential equation corresponds to each compartment.

4.5.1 Human Population

$\{S_h', E_h', I_{h1}', I_{h2}', A_h', R_h'\}$:

$S_h' = -ab\frac{I_v}{N_h}S_h - \beta\frac{\kappa E_h + I_{h1} + \tau I_{h2}}{N_h}S_h$

$E_h' = \theta[ab\frac{I_v}{N_h}S_h + \beta\frac{\kappa E_h + I_{h1} + \tau I_{h2}}{N_h}S_h] - \nu_h E_h$

$I_{h1}' = \nu_h E_h - \lambda_{h1} I_{h1}$

$I_{h2}' = \lambda_{h1} I_{h1} - \lambda_{h2} I_{h2}$

$A_h' = (1-\theta)[ab\frac{I_v}{N_h}S_h + \beta\frac{\kappa E_h + I_{h1} + \tau I_{h2}}{N_h}S_h] - \lambda_h A_h$

$R_h' = \lambda_{h2} I_{h2} + \lambda_h A_h,$

with initial conditions $S_h[0] = N_h$ and $E_h[0] = I_{1h}[0] = I_{h2}[0] = A_h[0] = R_h[0] = 0.$

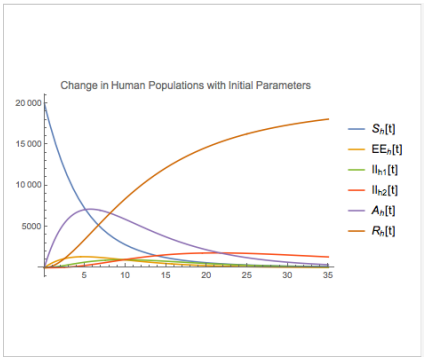

Figure 9: Model of the rates of change in human population with parameters set to initial estimates.

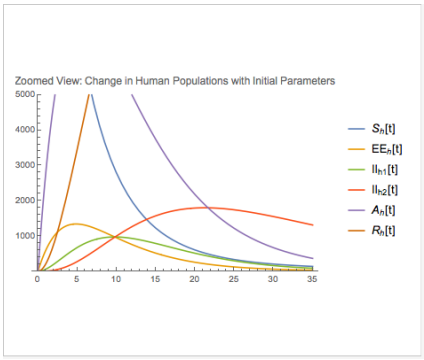

Figure 10: Model of the rates of change in human population with parameters set to initial estimates: a close view.

4.5.2 Mosquito Population

$\{S_v', E_v', I_v'\}$:

$S_v' = \mu_v N_v - ac\frac{\eta E_h + I_{h1}}{N_h}S_v - \mu_v S_v$

$E_v' = ac\frac{\eta E_h + I_{h1}}{N_h}S_v - (\nu_v + \mu_v)E_v$

$I_v' = \nu_v E_v - \mu_v I_v,$

with initial conditions $S_v[0] = \frac{3}{5}N_v$, $E_v[0] = \frac{1}{5}N_v$, and $I_v[0] = \frac{1}{5}N_v$.

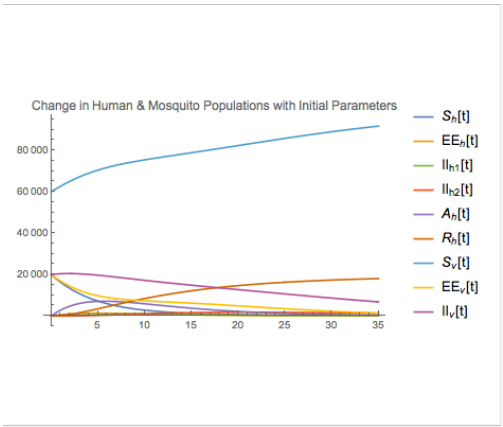

Figure 11: Model of the rates of change in human and mosquito populations with parameters set to initial estimates.

4.6 Evaluation of Parameters

We will discuss the individual impact of adjusting each parameter value.

a: Mosquito biting rate, with initial value .5 in range $[.3, 1]$

Mitigating the value of a reduces the rate of change of the susceptible human population. When $a = 0$, all humans remain susceptible as none become infected. As a grows larger, more and more susceptible individuals become exposed and eventually infected. As a grows closer to 1, the number of infected individuals significantly increases. Thus we strive for the value of a to be as close to 0 as possible.

b: Transmission probability from an infectious mosquito to a susceptible human per bite, with initial value .4 in range $[.1, .75]$

In an essentially identical way to a, mitigating the value of b diminishes the impact of ZIKV on the susceptible human population; when $b = 0$, all humans remain susceptible as none become infected. We also strive for the value of b to be as close to 0 as possible.

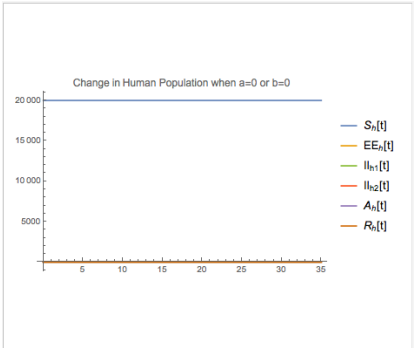

Figure 12: Change in Human Population when the Mosquito Biting Rate is 0 or the Transmission Probability from an Infectious Mosquito to a Susceptible Human is 0

c: Transmission probability from a symptomatically infected human to a susceptible mosquito per bite, with initial value .5 in range $[.3, .75]$

Changing the value of c moderately impacts the human population; a higher c value indirectly leads to more Zika infections – with humans leaving the susceptible population. A higher c value, too, leads to a greater amount of mosquitoes transitioning from susceptible to exposed and infectious. Changing c impacts the system on a small scale.

η: Relative human-to-mosquito transmission probability of exposed humans to susceptible mosquitoes, with initial value .2 in range $[0, .3]$

Changing the value of η impacts both the human and the mosquito population in a similar way to changing the value of c. However, a change in η has a lesser impact than a change in c, indicating that humans showing symptoms are more contagious to mosquitoes than humans who have been exposed to the virus.

β: Transmission rate from symptomatically infected humans to susceptible humans per day, with initial value .05 in range $[.001, .1]$

Increasing the value of β causes the susceptible population to diminish at a faster rate as more humans are infected through sexual transmission. However, this impact is minimal. The β value is estimated at .05, and when $\beta = .05$, the impact on the system is only slightly different than when sexual transmission is removed altogether ($\beta = 0$). Even when the sexual transmission rate is as high as possible ($\beta = 1$), which is much higher than the real value, the effect on the susceptible human population is more significant but still not drastic. This indicates that sexual transmission is not a primary means of transmission of ZIKV.

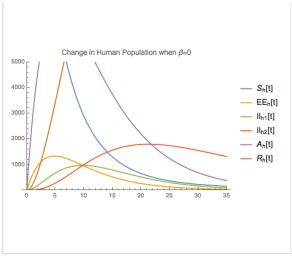

Figure 13: Sexual transmission rate is 0; Sexual transmission has no role.

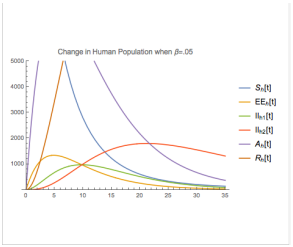

Figure 14: Sexual transmission rate is .05.

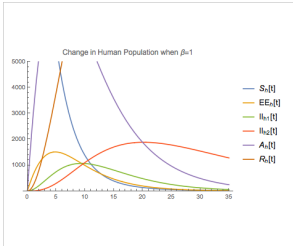

Figure 15: Sexual transmission rate is 1.

κ: Relative human-to-human transmissibility of exposed humans to susceptible humans, with initial value .6 in range $[0, 1]$

A nonzero β value is necessary for κ (or τ) to impact the system at all. If humans showing symptoms cannot affect the susceptible population, then those who are still in the incubation period and those who are recovering certainly cannot. The impact of κ is very small, leading to a slightly more rapid decline in the susceptible human population when κ is as high as possible (κ=1).

τ: Relative human-to-human transmissibility of convalescent humans to susceptible humans, with initial value .3 in range $[0, 1]$

The impact of τ, while also causing the susceptible human population to diminish more quickly, is extremely minor even when τ is as high as possible (τ=1). While neither κ nor τ greatly impact the system, changing κ has more significant results.

θ: Proportion of symptomatic infections, expressed as a percentage,with initial value .18 in range $[.1, .27]$

Even small changes in the θ value impact the system. As the value of θ increases, the susceptible human population declines at a faster rate, and the size of the asymptomatically infected population grows smaller as more and more humans move into the symptomatically infected population. As asymptomatic humans cannot infect other humans while symptomatic humans can, the epidemic grows more prevalent when θ is large, heightening the exposed population as well as the convalescent population – in addition to the symptomatically infected population. While the estimated range for θ values is .1 to .27 and realistically all infections would never be symptomatic (θ=1), the drastic changes depicted in the third figure demonstrate how significant this parameter is. Thus we hope for θ to be as small as possible to improve the dangers of exposition to ZIKV as well as to limit the spread of the virus.

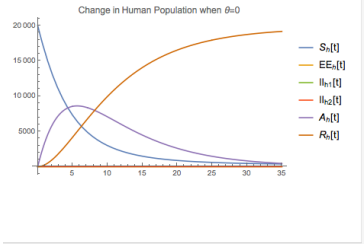

Figure 16: Change in Human Population when the proportion of symptomatic infections is 0; All infections are asymptomatic.

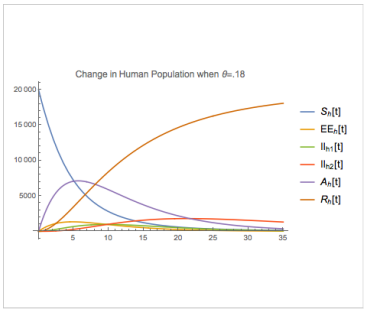

Figure 17: Change in Human Population when the proportion of symptomatic infections is .18; This is the real estimated value of θ.

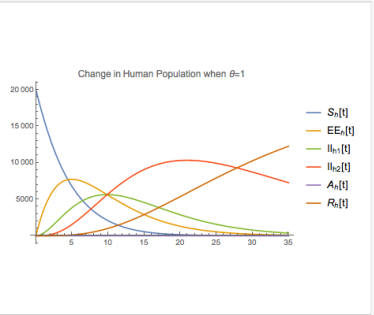

Figure 18: Change in Human Population when the proportion of symptomatic infections is 1; All infections are symptomatic.

ν_h: Intrinsic incubation rate in humans, measured in $\frac{1}{days}$, with initial value $\frac{1}{5}$ in range $[\frac{1}{7}, \frac{1}{2}]$
Adjusting the value of ν_h changes the amount of time it takes for exposed humans to enter the asymptomatically and symptomatically infected populations. A smaller ν_h value (corresponding to a longer span for the incubation period) causes the exposed population to peak at the beginning of the epidemic, delaying growth in the two infected populations.

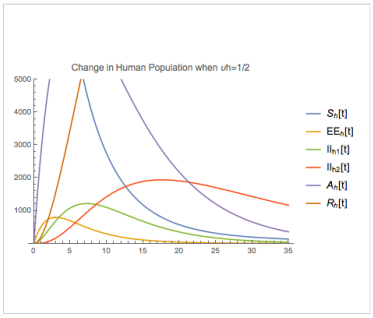

Figure 19: Change in Human Population when the human incubation rate is 1/2; Humans are incubated in 2 days.

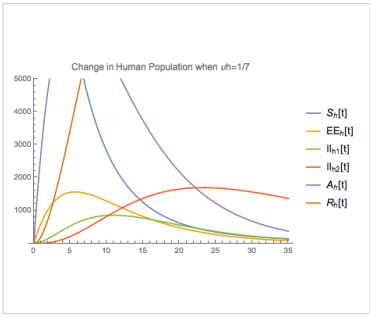

Figure 20: Change in Human Population when the human incubation rate is 1/7; Humans are incubated in 7 days.

ν_v: Extrinsic incubation rate in mosquitoes, measured in $\frac{1}{days}$, with initial value $\frac{1}{10}$ in range $[\frac{1}{12}, \frac{1}{8}]$
As ν_v grows smaller (corresponding to a longer span for the incubation period), the rate of change of the infectious mosquito population grows smaller as the exposed mosquito population grows larger. Additionally, the susceptible human population declines at a slightly slower rate when ν_v is small.

λ_{h1}: Rate of acute phase, measured in $\frac{1}{days}$, with initial value $\frac{1}{5}$ in range $[\frac{1}{7}, \frac{1}{3}]$
With a lower value of λ_{h1} (corresponding to a longer span for the acute phase), the symptomatically infected human population shows more growth and sustains growth for longer, delaying the entry of those with symptomatic infections into the convalescent population – and additionally delaying their eventual entry into the recovered population. A higher λ_{h1} value also causes a slight decrease in the susceptible human population, indicating that humans in the acute phase are more likely to infect others than humans than those in the convalescent phase – showing that symptomatic humans are more contagious.

λ_{h2}: Rate of convalescent phase, measured in $\frac{1}{days}$, with initial value $\frac{1}{20}$ in range $[\frac{1}{30}, \frac{1}{14}]$
The convalescent human population grows at a steady rate for the first days of the outbreak, at which point the value of λ_{h2} impacts its rate of change. With a lower value of λ_{h2} (corresponding to a longer span for the convalescent phase), the convalescent human population reaches a higher peak, and individuals remain in this population for longer – delaying their entry into the recovered population.

λ_h: Rate of asymptomatic infection, measured in $\frac{1}{days}$, with initial value $\frac{1}{7}$ in range $[\frac{1}{10}, \frac{1}{5}]$
With a lower value of λ_h (corresponding to a longer span for an asymptomatic infection), the asymptomatically infected human population demonstrates more growth and sustains higher proportions of individuals

during the outbreak, delaying the transition of humans from the asymptomatically infected population to the recovered population.

μ_v: Rate of mosquito lifespan, measured in $\frac{1}{days}$, with initial value $\frac{1}{14}$ in range $[\frac{1}{35}, \frac{1}{4}]$

A change in μ_v significantly impacts the system. With a higher value of μ_v (corresponding to a shorter mosquito lifespan), the susceptible human population declines at a drastically slower rate, and ZIKV impacts a much smaller amount of the total human population. When μ_v is small, the susceptible human population declines rapidly, causing great increases in every other population, as individuals progress out of the susceptible category into other populations. The growth of the susceptible mosquito population, too, is reduced significantly with a high value of μ_v – as the lives of mosquitoes are very short.

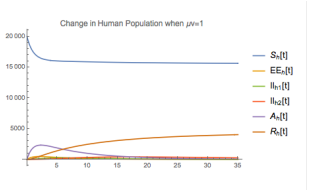

Figure 21: Change in Human Population when the mosquito lifespan rate is 1; Mosquito lifespan is only 1 day.

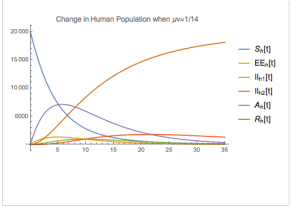

Figure 22: Change in human population when the mosquito lifespan rate is 1/14; Mosquito lifespan is 14 days.

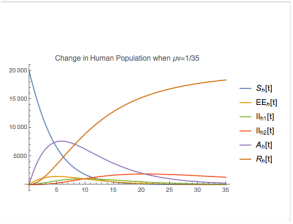

Figure 23: Change in Human Population when the mosquito lifespan rate is 1/35; Mosquito lifespan is 35 days.

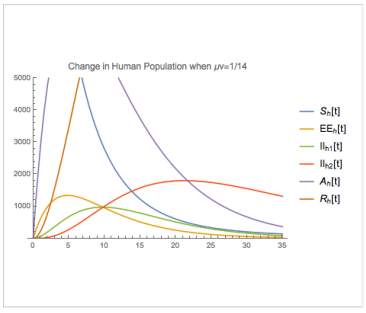

Figure 24: A close view of the change in the human population when the mosquito lifespan rate is 1/14.

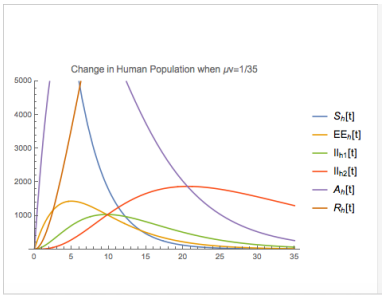

Figure 25: A close view of the change in the human population when the mosquito lifespan rate is 1/35.

5 Vaccination

5.1 Vaccine Development for ZIKV

Ever since the recognition of the severity of the ZIKV outbreak in 2015, vaccine development for this disease has been taken seriously, enduring as an active research project for many [2, 19]. Genomic sequences of the virus have been isolated from Brazil, and viral genes have been duplicated in order to work toward the creation of an effective vaccine which protects against contracting ZIKV [2]. In February of 2017, the World Health Organization (WHO) and the United Nations Children's Fund (UNICEF) collaborated to publish a Target Product Profile (TPP) for such a vaccine, designed for use by developers, procurement and regulatory agencies, and beneficiaries of immunization research and world health concerns [20]. At least 45 candidates for a ZIKV vaccine have been proposed – at least 25 of which have entered into nonclinical development and at least 9 of which are under clincial assessment [2].

Currently, the National Institute of Allergy and Infectious Diseases (NIAID) is working on the following 6 types of vaccines [18]: a DNA-based vaccine similar to an exploratory vaccine which protects against the West Nile virus, a purified inactivated vaccine similar to vaccines which have been created to protect against the associated dengue and Japanese encephalitis viruses, an exploratory weakened live vaccine which is composed of a genetically-engineered chimeric virus – comprised of a combination of genetic materials

from different viruses, exploratory mRNA vaccines similar to DNA-based vaccines, a multipurpose vaccine which includes four salivary gland synthetic proteins of mosquitoes and is intended to prevent infections with multiple viruses transmitted by mosquitoes, and finally an exploratory vaccine which contains a genetically-engineered variety of the vesicular stomatitis virus (VSV) which was utilized in the development of an effective exploratory Ebola vaccine.

In vaccine development, a vaccine may be *live* or *passive*, indicating the type of immunity that the vaccine confers [10]. Live vaccines correspond to active immunity, in which a dead or inactivated version of a disease-causing organism is introduced through vaccination, stimulating an immune response which generates the antibodies that protect a person from contracting that disease. So if an immune person is exposed to the full-strength virus, their immune system instantly induces the antibodies necessary to suppress the disease. On the other hand, passive vaccines confer passive immunity, in which the antibodies to fight a disease are directly introduced through vaccination. Hence, passive immunity is automatic upon vaccination, while active immunity develops over time as a person's immune system works to build up antibodies to a disease – but this type of immunity is much more enduring than the passive kind, and in some cases is even permanent [10].

5 of the 6 NIAID vaccine candidates are live rather than passive – all but the purified inactivated vaccine. Thus, we note that it is most realistic that a successful ZIKV vaccine will be live, but we still consider passive vaccination in our analysis of the effectiveness of a vaccination strategy.

5.2 Extending the Initial Model

5.2.1 A Live Vaccine

We now consider the impact of a live ZIKV vaccine on the transmission dynamics of the disease. Expanding the model of vectorial and sexual transmission of ZIKV [7], we apply vaccination to this system and build a new model. We assume that the vaccine confers permanent immunity to ZIKV but that it is not effective immediately, as it is live and thus yields active immunity. So, we introduce the following parameters:

ω: Vaccination rate, representing the proportion of the susceptible population (at t) vaccinated per day

ψ: Rate of phase of vaccine ineffectiveness, measured in $\frac{1}{days}$.

So the new model depends on the following set of parameters: $\{a, b, c, \eta, \beta, \kappa, \tau, \theta, \nu_h, \nu_v, \lambda_{h1}, \lambda_{h2}, \lambda_h, \mu_v, \omega, \psi\}$. Initially, ω is estimated at .02, corresponding to 2% of the susceptible population becoming vaccinated each day. ψ is estimated at 1/14, corresponding to a 14-day period of vaccine ineffectiveness, since live vaccines generally become functional after $1 - 3$ weeks [15].

Then, we modify the set of compartments which comprise the human population, appending the following:

V_{h1} represents the vaccinated susceptible individuals (in the phase of vaccine ineffectiveness), and

V_{h2} represents the vaccinated immune individuals (beyond the phase of vaccine ineffectiveness).

Hence, $N_h = S_h + E_h + I_{h1} + I_{h2} + A_h + V_{h1} + V_{h2} + R_h$.

Incorporating the new compartments and depicting their relationships with the pre-existing populations, Figure 26 displays the modified flow diagram for the live vaccination model. Recall that red nodes refer to infectious populations and green nodes refer to non-infectious populations. The new blue nodes refer to the vaccinated populations, which are also non-infectious. Recall, too, that blue arrows depict potential tracks for individuals as ZIKV spreads, black dashed arrows correspond to transmission among humans, and red dashed-dotted lines correspond to transmission among humans and mosquitoes.

Thus, individuals within V_{h1} may be infected by contact with the I_v, E_h, I_{h1}, or I_{h2} populations, at which point they move into E_h if their infection will be symptomatic or into A_h if their infection will be asymptomatic. Members of V_{h1} are susceptible to ZIKV until the the vaccine becomes effective; at this point, they can no longer contract the disease and progress into V_{h2} with lasting immunity. Importantly, V_{h2} constitutes a second possible endpoint for the human population. Therefore, individuals may conclude their passage through compartments in either V_{h2} or R_h.

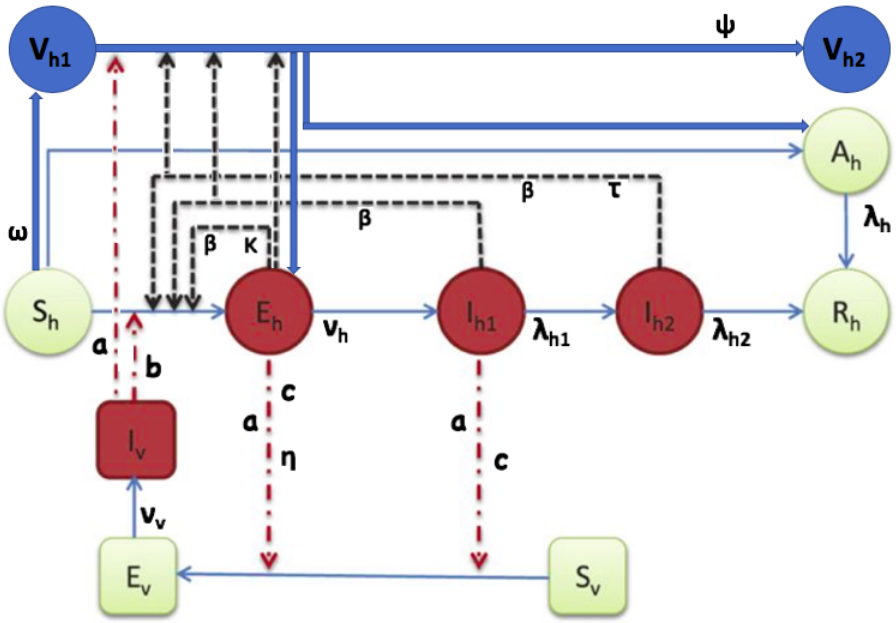

Figure 26: Flow Diagram for Transmission of ZIKV, with Both Vectorial and Sexual Modes, in the Presence of a Live Vaccine. This diagram is extended from [7].

This model now contains 11 ordinary differential equations, 8 describing the population dynamics of humans and the same 3 describing the population dynamics of mosquitoes.
Recalling that ω represents the vaccination rate for susceptible humans and ψ represents the rate of the phase of vaccine ineffectiveness, we adjust the differential equations for the human population as follows:

$$S_h' = -ab\frac{I_v}{N_h}S_h - \beta\frac{\kappa E_h + I_{h1} + \tau I_{h2}}{N_h}S_h - \omega S_h$$
$$E_h' = \theta[ab\frac{I_v}{N_h}S_h + \beta\frac{\kappa E_h + I_{h1} + \tau I_{h2}}{N_h}S_h] + \theta[ab\frac{I_v}{N_h}V_{h1} + \beta\frac{\kappa E_h + I_{h1} + \tau I_{h2}}{N_h}V_{h1}] - \nu_h E_h$$
$$I_{h1}' = \nu_h E_h - \lambda_{h1} I_{h1}$$
$$I_{h2}' = \lambda_{h1} I_{h1} - \lambda_{h2} I_{h2}$$
$$A_h' = (1-\theta)[ab\frac{I_v}{N_h}S_h + \beta\frac{\kappa E_h + I_{h1} + \tau I_{h2}}{N_h}S_h] + (1-\theta)[ab\frac{I_v}{N_h}V_{h1} + \beta\frac{\kappa E_h + I_{h1} + \tau I_{h2}}{N_h}V_{h1}] - \lambda_h A_h$$
$$V_{h1}' = \omega S_h - [ab\frac{I_v}{N_h}V_{h1} + \beta\frac{\kappa E_h + I_{h1} + \tau I_{h2}}{N_h}V_{h1}] - \psi V_{h1}$$
$$V_{h2}' = \psi V_{h1}$$
$$R_h' = \lambda_{h2} I_{h2} + \lambda_h A_h.$$

5.2.2 A Passive Vaccine

We now consider the influence of a passive ZIKV vaccine within the system. The vaccine becomes effective immediately upon vaccination, so there is no need for a rate of the phase of vaccine ineffectiveness ψ or a second vaccinated compartment V_{h2}. Thus, we modify the live vaccination model to represent transmission dynamics of ZIKV in the presence of passive vaccination, with only one vaccinated compartment V_h. The assumption that the vaccine confers permanent immunity to the disease remains. See Figure 27 for an updated flow diagram for the passive vaccination model.

Under such conditions, upon entering V_h individuals are instantly immune to infection with ZIKV with permanent immunity. If vaccinated, individuals simply move from S_h to V_h, with no possibility of eventual entry into R_h.

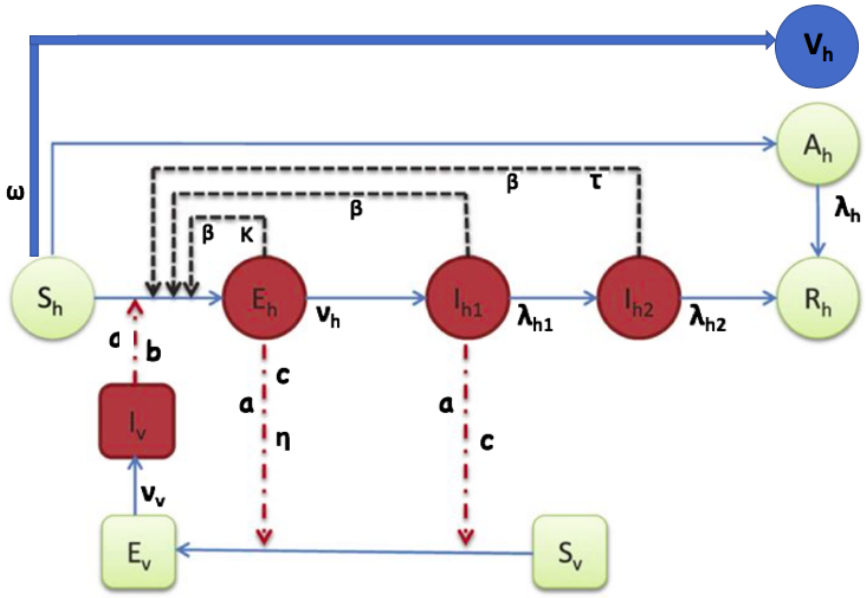

Figure 27: Flow Diagram for Transmission of ZIKV, with Both Vectorial and Sexual Modes, in the Presence of a Passive Vaccine. This diagram is extended from [7].

This model now contains 10 ordinary differential equations, 7 describing the population dynamics of humans and the same 3 describing the population dynamics of mosquitoes.
We adjust the differential equations for the passive vaccination model as follows:

$S_h' = -ab\frac{I_v}{N_h}S_h - \beta\frac{\kappa E_h + I_{h1} + \tau I_{h2}}{N_h}S_h - \omega S_h$
$E_h' = \theta[ab\frac{I_v}{N_h}S_h + \beta\frac{\kappa E_h + I_{h1} + \tau I_{h2}}{N_h}S_h] + \theta[ab\frac{I_v}{N_h}V_{h1} + \beta\frac{\kappa E_h + I_{h1} + \tau I_{h2}}{N_h}V_{h1}] - \nu_h E_h$
$I_{h1}' = \nu_h E_h - \lambda_{h1} I_{h1}$
$I_{h2}' = \lambda_{h1} I_{h1} - \lambda_{h2} I_{h2}$
$A_h' = (1-\theta)[ab\frac{I_v}{N_h}S_h + \beta\frac{\kappa E_h + I_{h1} + \tau I_{h2}}{N_h}S_h] + (1-\theta)[ab\frac{I_v}{N_h}V_{h1} + \beta\frac{\kappa E_h + I_{h1} + \tau I_{h2}}{N_h}V_{h1}] - \lambda_h A_h$
$V_h' = \omega S_h$
$R_h' = \lambda_{h2} I_{h2} + \lambda_h A_h.$

6 Results

We evaluate the following strategies for control of ZIKV transmission:

6.1 Live Vaccination

The presence of a live vaccine within a population susceptible to ZIKV has the potential to completely eradicate transmission of the disease, with time being the crucial factor. If the entire population has been vaccinated and has become immune to ZIKV before introduction of the virus, it is impossible for the disease to affect the community, and transmission dynamics progress from the no-vaccine state in Figure 28 to the disease-free state in Figure 29 – with all humans occupying V_{h2}, shown in yellow.

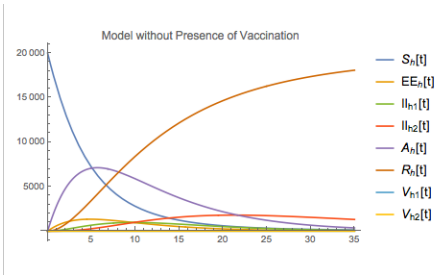

Figure 28: Model Behavior before Introduction of Vaccine, with Parameters set to Initial Estimates

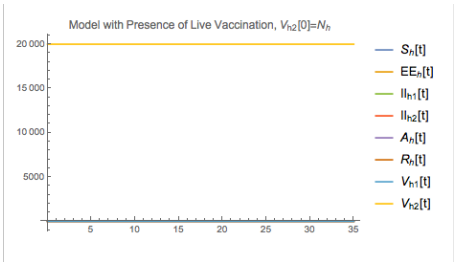

Figure 29: Model Behavior in Presence of Live Vaccine, with Entire Human Population Immune in Advance of ZIKV Introduction

Realistically, complete immunization of the population is infeasible. Even if the ZIKV vaccine could be made accessible to the entire population, vaccines are too dangerous for certain vulnerable individuals who may be too sick or too young to safely receive a vaccine. Some also question the risks associated with vaccines and may choose not to vaccinate themselves and their children [15]. However, the closer a population becomes to total vaccination before the start of an outbreak, the closer the spread of ZIKV becomes to this ideal state, as the potential impact of ZIKV gradually declines further and further. Figures $30 - 33$ demonstrate the progression of transmission dynamics as the proportion of the population that has become vaccinated against and immune to ZIKV grows larger and larger, with all parameters held constant at initial estimates.

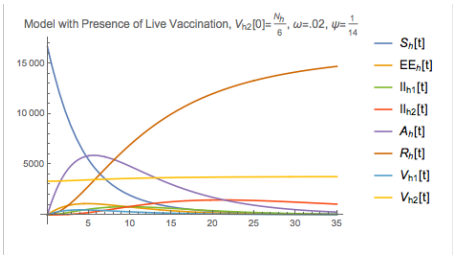

Figure 30: Model Behavior in Presence of Live Vaccine, with $\frac{1}{6}$ Human Population Immune in Advance of ZIKV Introduction

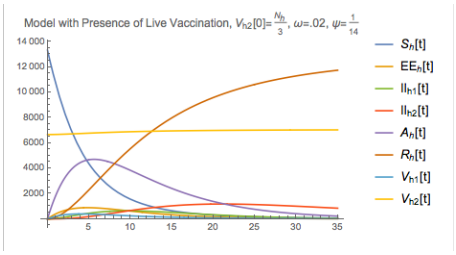

Figure 31: Model Behavior in Presence of Live Vaccine, with $\frac{1}{3}$ Human Population Immune in Advance of ZIKV Introduction

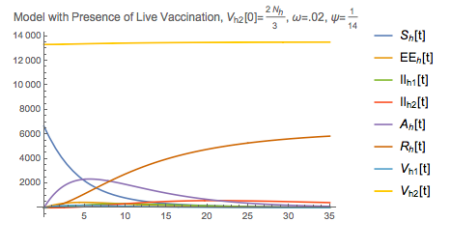

Figure 32: Model Behavior in Presence of Live Vaccine, with $\frac{2}{3}$ Human Population Immune in Advance of ZIKV Introduction

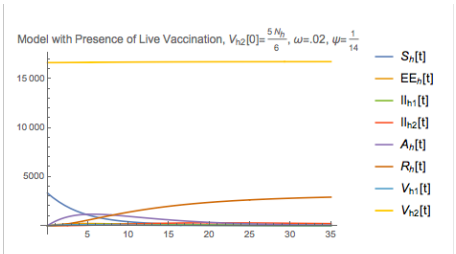

Figure 33: Model Behavior in Presence of Live Vaccine, with $\frac{5}{6}$ Human Population Immune in Advance of ZIKV Introduction

According to these simulations, pipe-lining individuals into the immune compartment V_{h2} before an outbreak begins evidently decreases the susceptible human population at $t = 0$ and reduces the amount of total humans impacted by ZIKV at a rate inversely proportional to the amount of humans in $V_{h2}[0]$. However, the nature of the differential curves of the infected human populations $\{E_h, I_{h1}, I_{h2}\}$ changes only slightly with small changes to $V_{h2}[0]$, with crucial differences occurring only when more than half of the human population is immune to ZIKV at $t = 0$, with $V_{h2}[0] > \frac{1}{2}N_h$. Figures 30 and 31 display rates of

change similar to no-vaccination conditions in Figure 28, while Figures 32 and 33 demonstrate gross reduction in ZIKV transmission. As the yellow curve grows closer and closer to $20,000$, $V_{h2}[0] \to N_h$, and model behavior approaches the ideal conditions of Figure 29.

Taking a closer look at Figure 30, when only $\frac{1}{6}th$ of the susceptible human population is immune to ZIKV at $t = 0$, the differential curves demonstrate a lesser effect of ZIKV than the no-vaccine conditions of Figure 28 – but to a very minimal degree. Figures 28 and 30 show slight differences in the rates of change of $\{E_h, I_{h1}, I_{h2}\}$, but these changes are difficult to see without zooming in on the graphs. Figures 34 and 35 display these figures in range $[1, 1000]$, demonstrating that vaccination in this scenario reduces the spike in I_{h1} by a factor of nearly $\frac{1}{5}th$ and scales down the outbreak as a whole as individuals move into V_{h1} and eventually into V_{h2}. However, this change in impact is inconsequential in the scope of an entire outbreak, with no real influence on its timescale.

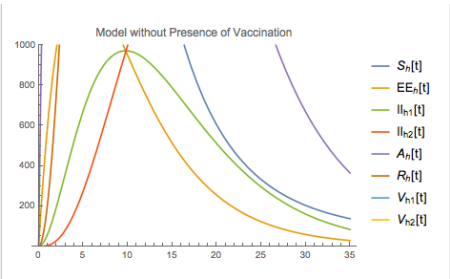

Figure 34: Model Behavior Before Introduction of Vaccine: A Close View.

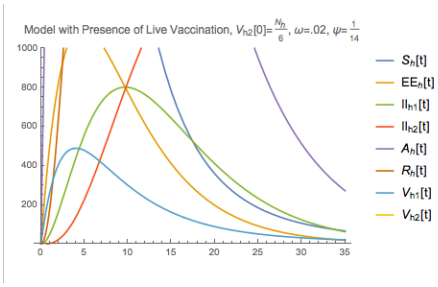

Figure 35: Model Behavior in Presence of Live Vaccine, with $\frac{1}{6}$ Human Population Immune in Advance of ZIKV Introduction: A Close View.

As the figures show, the disease advances through the population in essentially the same manner when $V_{h2}[0] = \frac{1}{6}N_h$ as when no vaccine is present in the system. Even with more vaccinations occurring every day, initially immunizing $\frac{1}{6}th$ of the human population is not enough to significantly limit transmission of the disease; there are still too many susceptible humans in $\{S_h, V_{h1}\}$ who interact with carriers of ZIKV and contract the disease.

Thus during a period when ZIKV is not an immediate threat to a community, preemptive vaccination is key. On the same small scale of $[1, 1000]$, Figures $36 - 38$ zoom in on Figures $31 - 33$ and demonstrate a closer view of the progression of the model's behavior as an increasing amount of the human population becomes immune in advance of the introduction of ZIKV.

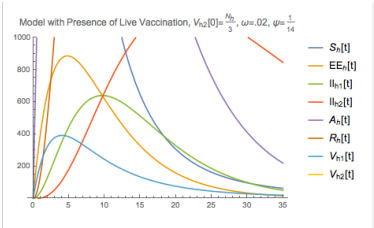

Figure 36: $V_{h2}[0] = \frac{1}{3}N_h$.

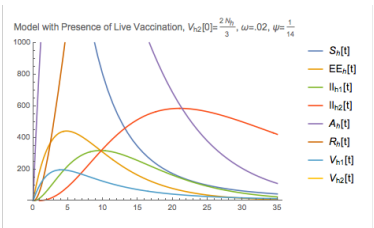

Figure 37: $V_{h2}[0] = \frac{2}{3}N_h$.

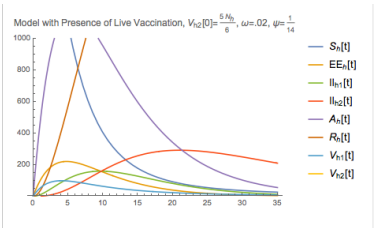

Figure 38: $V_{h2}[0] = \frac{5}{6}N_h$.

These results emphasize the inversely proportional relationship between $V_{h2}[0]$ and the influence of an outbreak – measured by the sizes of the infected populations $\{E_h, I_{h1}, I_{h2}\}$ as t increases. By the time that $V_{h2}[0]$ becomes as large as $\frac{5}{6}N_h$, the peak of I_{h1} has been reduced by approximately $\frac{5}{6}th$ of its original size. This change reflects how successful a vaccination strategy may be in controlling and even preventing outbreaks of ZIKV.

However, $V_{h2}[0]$ is the paramount value. Once an outbreak has already begun its course and $t \neq 0$, vaccinating the susceptible population as quickly as possible may alleviate the outbreak but can only have

a minimal impact, as ZIKV spreads rapidly and we assume the live vaccine takes $1-3$ weeks to become effective. With parameters set to initial values, beginning a vaccination strategy after $t=0$ yields results similar to no-vaccine conditions. As Figures 39 and 40 demonstrate, both the full plot range and the close-up view of transmission dynamics in the presence of a vaccine with $V_{h2}[0]=0$ are incredibly similar to Figures 28 and 34, respectively. Once the vaccine has been introduced, the susceptible human population S_h diminishes at a slightly faster rate than in the presence of no immunization, as individuals move through V_{h1} and eventually into V_{h2} with immunity. However, with vaccination beginning after $t=0$, only a small proportion of the population is positively impacted by immunization. As Figure 40 indicates, at $t=35$, only 2.6% of the population has become immune by vaccination, with $V_{h2}[35] \approx 525 = .026N_h$. In addition, Figure 40 reflects that the differential dynamics of the infectious populations $\{E_h, I_{h1}, I_{h2}\}$ show only negligible differences from Figure 34. In Figure 40, I_{h1} peaks only 1% lower than no-vaccine conditions, with $I_{h1}[10] \approx 960$ in Figure 40 and $I_{h1}[10] \approx 970$ in Figure 34, indicating a slightly less severe outbreak than with the complete lack of immunization. Thus, while conditions in these two settings are not identical, the improvements in outbreak conditions are quite minimal.

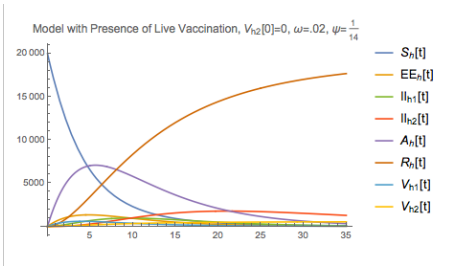

Figure 39: Model Behavior in Presence of Live Vaccine, with None of Human Population Immune in Advance of ZIKV Introduction, $\omega = .02$.

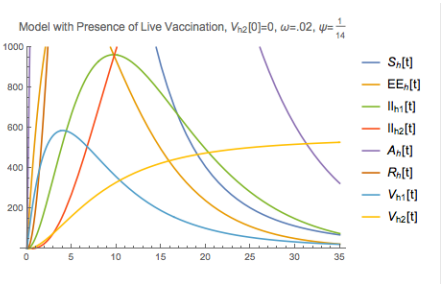

Figure 40: Model Behavior in Presence of Live Vaccine, with None of Human Population Immune in Advance of ZIKV Introduction, $\omega = .02$: A Close View.

Therefore, introducing a live vaccine into the system cannot consequentially ameliorate ZIKV transmission at this late stage (beyond $t=0$). Even if we adjust ω and ψ to optimal values, the maximum impact is severely limited.

First, we consider how a change in ω impacts the system, maintaining $V_{h2}[0]=0$ and holding all other parameter values unchanged. Ideally, a larger ω value will correspond to a lesser impact of a ZIKV outbreak, since a greater proportion of the susceptible population becomes vaccinated each day. However, as ω increases, variations in the rates of change of the infected populations $\{E_h, I_{h1}, I_{h2}\}$ are imperceptible on the large scale. The susceptible population S_h decreases at a significantly faster rate as more and more individuals become vaccinated, but the proportion of the population affected by immunization remains too small to improve transmission dynamics in a meaningful way. Figures $41-43$ display the striking lack of dissimilitude in the differential dynamics of $\{E_h, I_{h1}, I_{h2}, A_h, R_h\}$ as ω grows large.

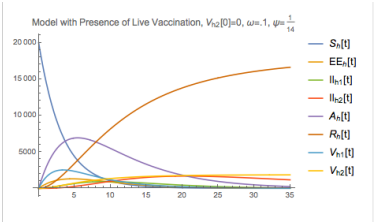

Figure 41: $\omega = .1$

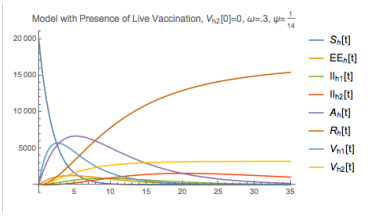

Figure 42: $\omega = .3$

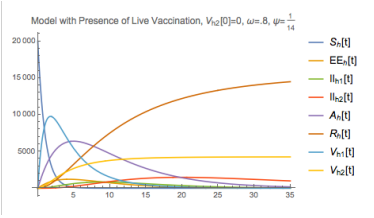

Figure 43: $\omega = .8$

As Figure 43 signifies, even when the percentage of the susceptible population vaccinated per day increases to 80%, with ω at the extreme value of .8, only $\frac{1}{5}th$ of the population has progressed into the V_{h2} compartment and has become immune to ZIKV by $t=35$, at which point the size of V_{h2} has been plateauing for about 20 days. Under these conditions, $\frac{4}{5}th$ of the total population is still affected by the

ZIKV outbreak in the same way as the no-vaccine state. Thus, with the full plot range, this figure reflects transmission dynamics of ZIKV which improve the conditions of Figure 39 only by a narrow margin.

However, even on the small scale, margins of change remain narrow. Figures $44 - 46$ display the progression of transmission dynamics in range $[0, 1000]$ as ω increases. As ω moves from .1 to .3 to .8, the peak of the growth of the infected population I_{h1} reduces only by approximately 4%, and the timescale of the outbreak shows no change. The susceptible population S_h diminishes at a more rapid rate as individuals become vaccinated and move into V_{h1} and V_{h2}, but these changes have such a small effect on the severity of the outbreak that the dynamics of the infectious populations $\{E_h, I_{h1}, I_{h2}\}$ virtually remain constant. Realistically, a value of $\omega = .8$ is almost certainly beyond reasonable limits for this parameter. So Figures 43 and 46 essentially display the maximum impact that adjustments in ω may yield, underscoring the insufficient impact of a vaccination strategy instituted after $t = 0$.

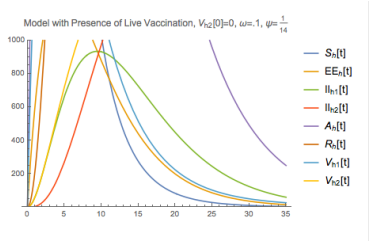

Figure 44: $\omega = .1$: A Close View.

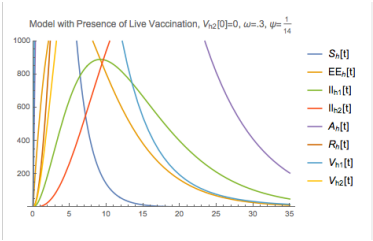

Figure 45: $\omega = .3$: A Close View.

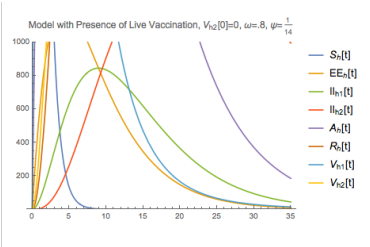

Figure 46: $\omega = .8$: A Close View.

Next, we consider how a change in ψ affects the system with no vaccination present until $t = 0$, with all other parameters held constant. As ψ increases, the number of days in which the vaccine remains ineffective decreases, and variations in the rates of change of $\{S_h, E_h, I_{h1}, I_{h2}, A_h, R_h\}$ are essentially nonexistent on the large scale. Figures $47 - 49$ indicate the lack of broad influence of whether the vaccine becomes effective within three, two, or one weeks. The curves are simply not distinguishable at the macro level.

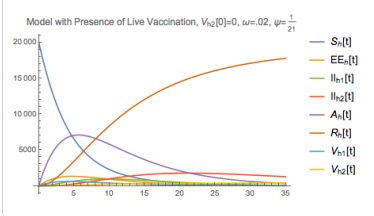

Figure 47: $\psi = \frac{1}{21}$, Vaccine Becomes Effective after 21 days.

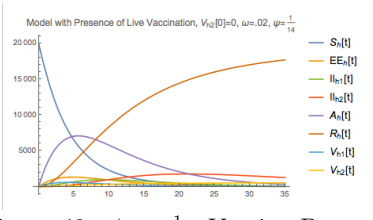

Figure 48: $\psi = \frac{1}{14}$, Vaccine Becomes Effective after 14 days.

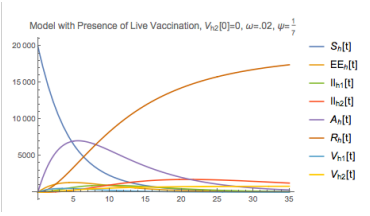

Figure 49: $\psi = \frac{1}{7}$, Vaccine Becomes Effective after 7 days.

On the micro level, changes remain minimal. Figures $50 - 52$ concentrate on the effect of changing ψ on the infectious populations $\{E_h, I_{h1}, I_{h2}\}$ and vaccinated populations $\{V_{h1}, V_{h2}\}$ in range $[0, 1000]$. In these figures, a close view of the progression of the light blue and yellow curves – representing the rates of change of V_{h1} and V_{h2} respectively – indicates that individuals move more quickly from V_{h1} into V_{h2}. In these figures, the impact of this progression is noteworthy, as approximately twice as many individuals have moved into V_{h2} at $t = 35$ in Figure 52 than in Figure 50. However, this progress is significant only on the small scale, as the vaccinated immune individuals in Figure 50 represent only approximately 2% of the total population while those in Figure 52 represent approximately 4% of the population, with $V_{h2}[35] \approx 400 = .02N_h$ when $\psi = \frac{1}{21}$ and $V_{h2}[35] \approx 800 = .04N_h$ when $\psi = \frac{1}{7}$. In addition, changes in the differential curves of $\{E_h, I_{h1}, I_{h2}\}$ are indiscernible even on this scale, reflecting the uniformity of large-scale transmission dynamics displayed in Figures $47 - 49$.

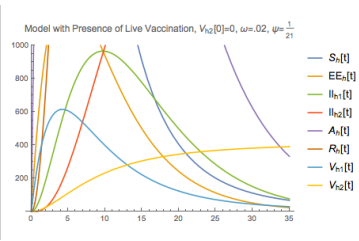

Figure 50: $\psi = \frac{1}{21}$, Vaccine Becomes Effective after 21 days: A Close View.

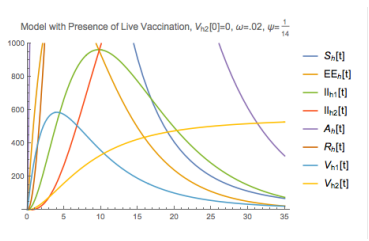

Figure 51: $\psi = \frac{1}{14}$, Vaccine Becomes Effective after 14 days: A Close View.

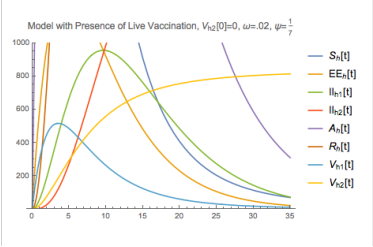

Figure 52: $\psi = \frac{1}{7}$, Vaccine Becomes Effective after 7 days: A Close View.

Thus in ideal conditions, ψ will be as large as possible, corresponding to the shortest possible period of vaccine ineffectiveness. Reducing this period may be feasible and depends completely on how the vaccine is developed. However, these graphs indicate that a larger ψ value has a negligible impact when a vaccination strategy is not instituted until after $t = 0$, reinforcing the preeminence of preemptive immunization measures, in line with the results of Figures $28 - 33$.

So, parameter adjustments in ω and ψ are insignificant when $V_{h2}[0] = 0$. However, as $V_{h2}[0] \to N_h$, could changes to ω and ψ have a greater influence on ZIKV infections? We consider this effect when $V_{h2}[0] = \frac{N_h}{6}$ and when $V_{h2}[0] = \frac{5N_h}{6}$.

Figures 53 and 54 recall transmission dynamics when $V_{h2}[0] = \frac{N_h}{6}$ in full range and in range $[1, 1000]$.

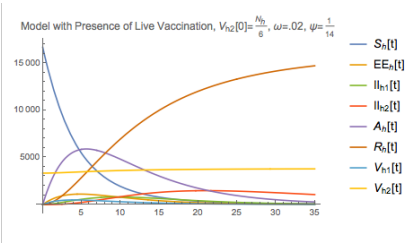

Figure 53: $\frac{1}{6}$ Human Population Immune in Advance of ZIKV Introduction, with Initial Conditions.

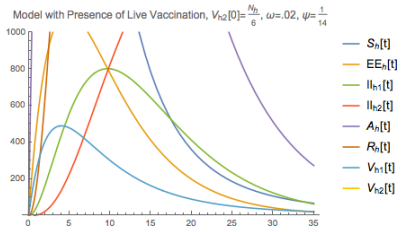

Figure 54: $\frac{1}{6}$ Human Population Immune in Advance of ZIKV Introduction, with Initial Conditions: A Close View.

Raising ω from .02 to .3 has a greater impact than raising ψ from $\frac{1}{14}$ to $\frac{1}{7}$, though both effects are minimal. If a serious vaccination strategy is instituted to vaccinate 30% of the susceptible population per day, setting $\omega = .3$ slightly reduces the severity of the ZIKV outbreak. On the large scale, a value of $\omega = .3$ causes approximately an additional 10% of the total population to become immune by vaccination by $t = 35$ than when $\omega = .02$, with $V_{h2}[35] \approx 4000$ in Figure 53 and $V_{h2}[35] \approx 6000$ in Figure 55, representing a total of approximately 30% of the entire population with immunity. But even with this 10% change, 70% of the total population is still affected by the ZIKV outbreak in the same way as under no-vaccination conditions. On the small scale, a value of $\omega = .3$ causes I_{h1} to peak approximately 8% lower and 1 day earlier than when $\omega = .02$, with $I_{h1}[10] \approx 800$ in Figure 54 and $I_{h1}[9] \approx 735$ in Figure 56. But these small-scale changes only affect approximately .3% of the total population at this peak.

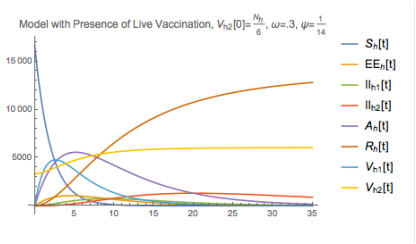

Figure 55: $\frac{1}{6}$ Human Population Immune in Advance of ZIKV Introduction, with $\omega = .3$.

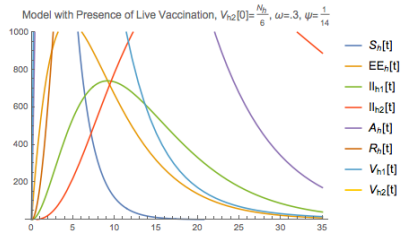

Figure 56: $\frac{1}{6}$ Human Population Immune in Advance of ZIKV Introduction, with $\omega = .3$: A Close View.

Therefore, a higher ω value does improve transmission dynamics of ZIKV, but the positive effect of increasing ω does not begin to compare to that of increasing $V_{h2}[0]$.

We now evaluate the effect of changing ψ from $\frac{1}{14}$ to $\frac{1}{7}$. As Figures 57 and 58 indicate, results are negligible.

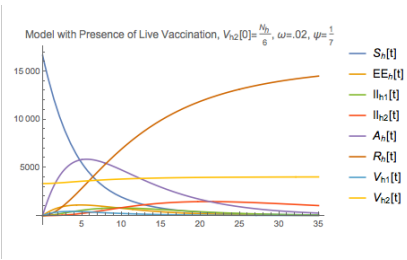

Figure 57: $\frac{1}{6}$ Human Population Immune in Advance of ZIKV Introduction, with $\psi = \frac{1}{7}$.

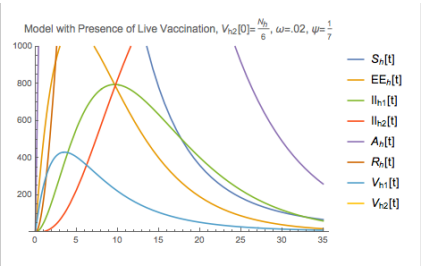

Figure 58: $\frac{1}{6}$ Human Population Immune in Advance of ZIKV Introduction, with $\psi = \frac{1}{7}$: A Close View.

On both the large and the small scale, the positive impact of reducing the period of vaccine ineffectiveness from 2 to 1 weeks is minimal to such an extent that differences are essentially imperceptible. In both Figures 57 and 53, $V_{h2}[35] \approx 4000$; and in both Figures 58 and 54, $I_{h1}[10] \approx 800$.

We now consider the influence of parameter adjustments when $V_{h2}[0] = \frac{5N_h}{6}$. Figures 59 and 60 recall transmission dynamics under these conditions in full range and in range $[1, 1000]$.

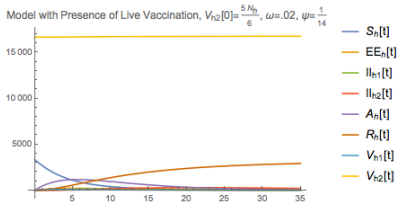

Figure 59: $\frac{5}{6}$ Human Population Immune in Advance of ZIKV Introduction, with Initial Conditions.

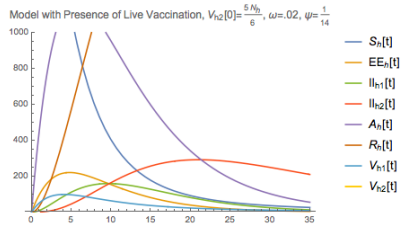

Figure 60: $\frac{5}{6}$ Human Population Immune in Advance of ZIKV Introduction, with Initial Conditions: A Close View.

Similarly to when $V_{h2}[0] = \frac{N_h}{6}$, raising ω and ψ yields minor results when $V_{h2}[0] = \frac{5N_h}{6}$, though a change in ω has a larger effect than a change in ψ. When $\omega = .3$ rather than .02, we observe slight improvements in transmission dynamics of ZIKV. On the large scale, this variation causes approximately an additional 2% of the total population to become immune as a result of vaccination by $t = 35$, with $V_{h2}[35] \approx 16,750$ in Figure 59 and $V_{h2}[35] \approx 17,150$ in Figure 61, with Figure 61 representing a total of approximately 86% of the entire population. Although certainly positive, this 2% change makes little difference in the scope of the entire outbreak. Zoning in on the small scale, a value of $\omega = .3$ causes I_{h1} to peak approximately 6%

lower and $\frac{1}{2}$ days earlier than when $\omega = .02$, with $I_{h1}[10] \approx 160$ in Figure 60 and $I_{h1}[9.5] \approx 150$ in Figure 62. On the large scale, these small-scale changes are insignificant, influencing only approximately .05% of the total population at this peak.

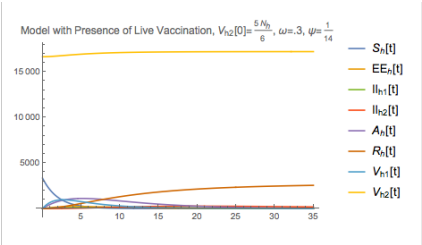

Figure 61: $\frac{5}{6}$ Human Population Immune in Advance of ZIKV Introduction, with $\omega = .3$.

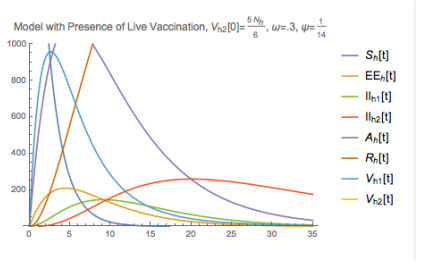

Figure 62: $\frac{5}{6}$ Human Population Immune in Advance of ZIKV Introduction, with $\omega = .3$: A Close View.

Thus, increasing ω still improves transmission dynamics of ZIKV when $V_{h2}[0] = \frac{5N_h}{6}$, but this effect is even less than increasing ω when $V_{h2}[0] = \frac{N_h}{6}$ – as these less ideal conditions allow for greater room for growth – and vastly less than an increase in $V_{h2}[0]$.

We now evaluate the effect of increasing ψ when $V_{h2}[0] = \frac{5N_h}{6}$. As Figures 63 and 64 convey, just like for $V_{h2}[0] = \frac{N_h}{6}$, results are trivial.

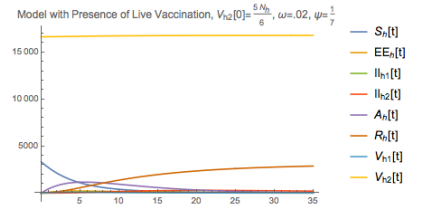

Figure 63: $\frac{5}{6}$ Human Population Immune in Advance of ZIKV Introduction, with $\psi = \frac{1}{7}$.

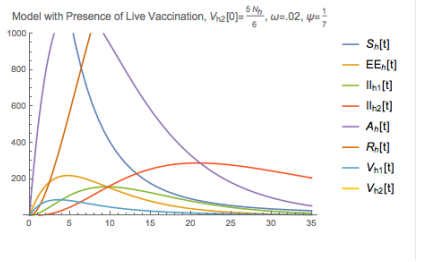

Figure 64: $\frac{5}{6}$ Human Population Immune in Advance of ZIKV Introduction, with $\psi = \frac{1}{7}$: A Close View.

Under conditions such that $V_{h2}[0] = \frac{5N_h}{6}$, the positive effect of minimizing the period of vaccine ineffectiveness from 2 to 1 weeks is undetectable both in range $[0, 18000]$ and $[0, 1000]$. In both Figures 63 and 59, $V_{h2}[35] \approx 16750$; and in both Figures 64 and 60, $I_{h1}[10] \approx 160$.

Hence, we have evaluated the impact of a live immunization strategy for controlling the spread of ZIKV with a specific focus on adaptations to the following set of quantities: $\{V_{h2}[0], \omega, \psi\}$. While increasing ψ has virtually no influence and increasing ω can yield only limited improvements to transmission dynamics, increasing $V_{h2}[0]$ has transformative power in immobilizing ZIKV. As $V_{h2}[0] \to N_h$, the impact of an outbreak reduces dramatically; the more individuals who become immune to ZIKV before the inception of an outbreak, the less transmittable the disease becomes. Therefore, the introduction of a live vaccine has the capability to control the gravity of an outbreak, with time serving as the determining factor. The practicality of this strategy depends on the viability of advance vaccinations for a large percentage of the population; for this solution to be effective, the immunization must be available for large quantities of people and accessible to essentially the entire population in terms of both affordability and location, and a high proportion of individuals must be willing to make it a priority to become vaccinated preemptively.

6.2 Passive Vaccination

The presence of a passive vaccine – like that of a live vaccine – has the capability to erase all transmission of ZIKV. However, since we are now considering passive immunity, time – while still important – is no longer

as critical. Regardless, if the entire human population becomes vaccinated and thus instantly immune to ZIKV before any exposure to it, it becomes impossible for the virus to influence the population at all. In this case, just like with live vaccination, population dynamics move from the no-vaccine conditions of Figure 65 to the disease-free conditions of Figure 66, with all humans occupying V_h – shown in light blue.

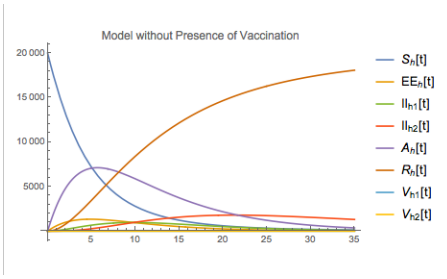

Figure 65: Model Behavior before Introduction of Vaccine, with Parameters set to Initial Estimates

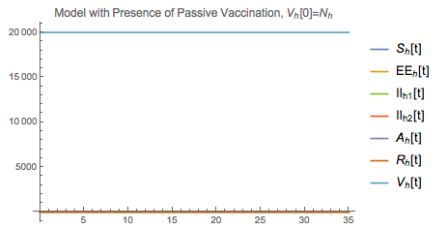

Figure 66: Model Behavior in Presence of Passive Vaccine, with Entire Human Population Immune in Advance of ZIKV Introduction

As we previously noted, the dynamics of Figure 66 are unattainable in real life, since absolute vaccination of the human population is unrealistic. But like with live vaccination, the closer a population moves toward total vaccination before an outbreak begins, the less ZIKV may strike the community. Figures $67 - 70$ display the variation in population dynamics as the vaccinated (and thus immune) population at $t = 0$ increases, with all parameters set to initial values.

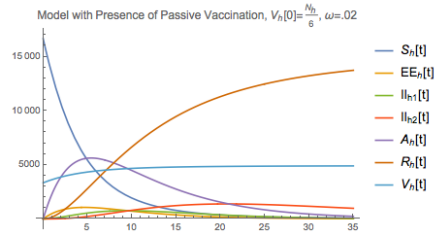

Figure 67: Model Behavior in Presence of Passive Vaccine, with $\frac{1}{6}$ Human Population Immune in Advance of ZIKV Introduction

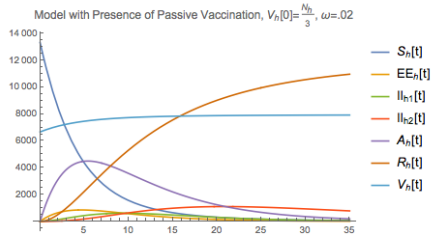

Figure 68: Model Behavior in Presence of Passive Vaccine, with $\frac{1}{3}$ Human Population Immune in Advance of ZIKV Introduction

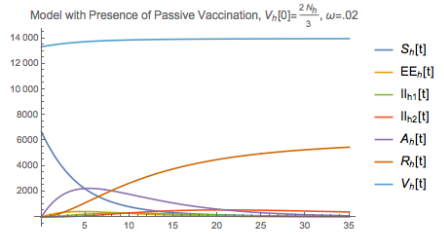

Figure 69: Model Behavior in Presence of Passive Vaccine, with $\frac{2}{3}$ Human Population Immune in Advance of ZIKV Introduction

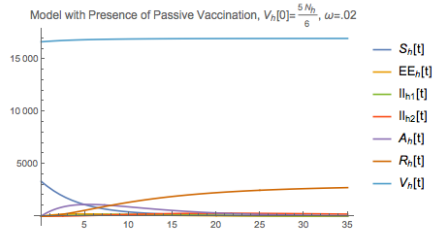

Figure 70: Model Behavior in Presence of Passive Vaccine, with $\frac{5}{6}$ Human Population Immune in Advance of ZIKV Introduction

Again in a similar fashion to live vaccination, advancing more and more individuals into the vaccinated compartment V_h before the start of a ZIKV outbreak diminishes the size of the susceptible population at $t = 0$ and lessens the influence of the outbreak at a rate inversely proportional to the size of $V_h[0]$. However, the immediate effectiveness of passive vaccination causes conditions most different from live

vaccination when $V_h[0]$ is small. Under such conditions, with a smaller proportion of the population initially immune to ZIKV and hence a greater number of susceptibles, the instant vaccine has greater space to be effective. While $V_{h2}[35] \approx 3500$ with a live vaccine when $V_{h2}[0] = \frac{1}{6}N_h$ (Figure 30), $V_h[35] \approx 5000$ under the same conditions but in the presence of a passive vaccine (Figure 67). As $V_h[0]$ grows, though, the impact of a passive versus an active vaccine approaches 0. When $V_h[0] = \frac{1}{3}N_h$, a live vaccine yields $V_{h2}[35] \approx 7000$ (Figure 31) while a passive vaccine yields only $V_h[35] \approx 7850$ (Figure 68); and when $V_h[0] = \frac{2}{3}N_h$, a live vaccine yields $V_{h2}[35] \approx 13250$ (Figure 32) while a passive vaccine yields $V_h[35] \approx 13950$ (Figure 69). And once $V_h[0] = \frac{5}{6}N_h$, both the live and the passive vaccine yield $V_{h2}[35] \approx V_h[35] \approx 17000$ (Figures 33 and 70). So if both passive and live vaccination confer permanent immunity, the two strategies have similar effectiveness at $V_h[0]$ grows large, but a passive vaccine demonstrates a greater impact when $V_h[0]$ is smaller. Thus, while a larger percentage of the population becoming vaccinated in advance of an outbreak always yields superior results, passive vaccination shows greater flexibility in regards to the time of immunization.

Zooming in to range $[1, 1000]$ mirrors these results. As Figures 71 and 72 demonstrate, an initial size of V_h of $\frac{1}{6}th$ of the susceptible population decreases the peak of I_{h1} by a factor of nearly $\frac{1}{4}th$, an only 5% more significant change than under conditions of live vaccination (See Figure 35).

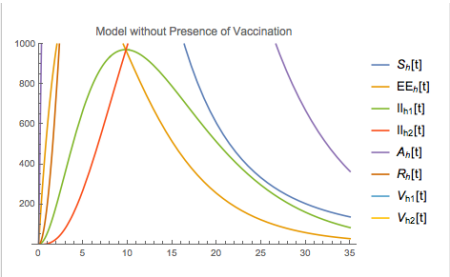

Figure 71: Model Behavior Before Introduction of Vaccine: A Close View.

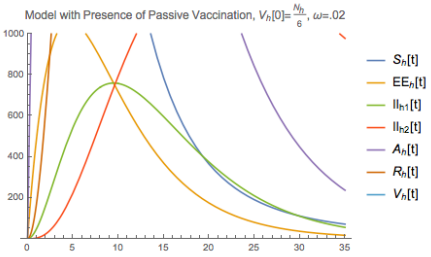

Figure 72: Model Behavior in Presence of Passive Vaccine, with $\frac{1}{6}$ Human Population Immune in Advance of ZIKV Introduction: A Close View.

Further, as N_h grows large, the variation in the results of passive and active immunization campaigns shrinks to virtually no change. When $V_h[0] = \frac{1}{3}N_h$, a live vaccine yields $I_{h1}[10] \approx 640$ (Figure 36) while a passive vaccine yields only $I_{h1}[10] \approx 600$ (Figure 73); and when $V_h[0] = \frac{2}{3}N_h$, a live vaccine yields $I_{h1}[10] \approx 310$ (Figure 37) while a passive vaccine yields $I_{h1}[10] \approx 300$ (Figure 74). Similarly, when $V_h[0] = \frac{5}{6}N_h$, a live vaccine yields $I_{h1}[10] \approx 160$ (Figure 38) while a passive vaccine yields $I_{h1}[10] \approx 150$ (Figure 75).

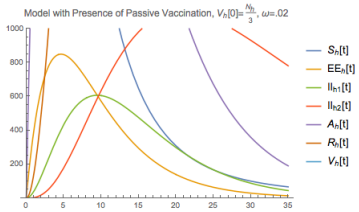

Figure 73: $V_h[0] = \frac{1}{3}N_h$.

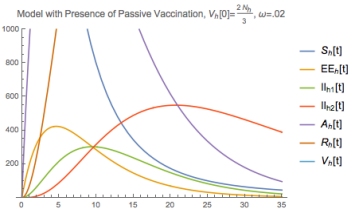

Figure 74: $V_h[0] = \frac{2}{3}N_h$.

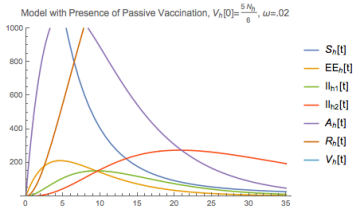

Figure 75: $V_h[0] = \frac{5}{6}N_h$.

Thus, these figures underscore the triviality of the distinction between a live and a passive vaccination strategy when $V_h[0]$ is large. But even when $V_h[0]$ is small, strategic passive vaccination improves transmission dynamics to only a slightly higher degree than live vaccination.

However, the key difference between active and passive immunization lies not in the value of $V_h[0]$ but in the value of ω. While a change in ω may yield only minimal results for a live vaccination strategy once an

outbreak has already commenced, a passive vaccination strategy – being less time-sensitive – is still able to have a crucial impact on the human population even if instituted after $t = 0$. Without the $1 - 3$ week period of vaccine ineffectiveness, mass passive immunization – if rapid enough – can show great success in combating ZIKV.

So, we consider the influence of adjusting ω in the presence of a passive vaccine when $V_h[0] = 0$. Figures 76 and 77 display both the full and close-up plot ranges of transmission dynamics under such conditions, with ω set the initial estimate of .02.

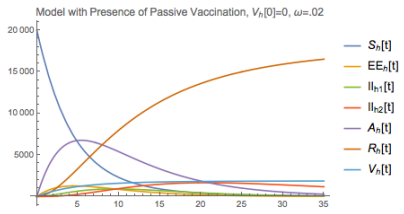

Figure 76: Model Behavior in Presence of Passive Vaccine, with None of Human Population Immune in Advance of ZIKV Introduction, $\omega = .02$.

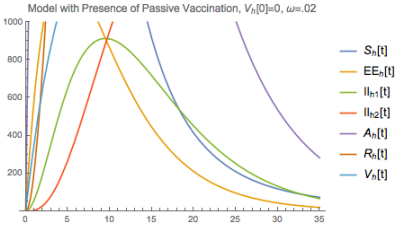

Figure 77: Model Behavior in Presence of Passive Vaccine, with None of Human Population Immune in Advance of ZIKV Introduction, $\omega = .02$: A Close View.

As Figure 76 shows, the number of immune individuals at $t = 35$ has grown to approximately 1900 – a noteworthy improvement over the 550 individuals at this time under live vaccination conditions (Figure 40). Figure 77, too, demonstrates a slight improvement in transmission dynamics, with the peak of the infectious population decreasing from $I_{h1}[10] \approx 960$ with live vaccination (Figure 40) to $I_{h1}[10] \approx 900$ with passive vaccination. While these improvements are certainly recognizable, the differential curves of Figures 76 and 77 remain quite similar to the live vaccination conditions of Figures 39 and 40 – and thus very similar to the no-vaccine conditions of Figures 28 and 34.

But, increasing ω further under conditions of passive immunization enacts prominent advances in controlling ZIKV. Figures $78 - 80$ display large-scale transmission dynamics as ω moves from .1 to .3 to .8 – showing striking changes from the conditions of active immunization in Figures $41 - 43$.

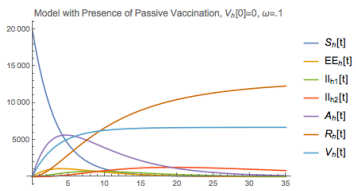

Figure 78: $\omega = .1$

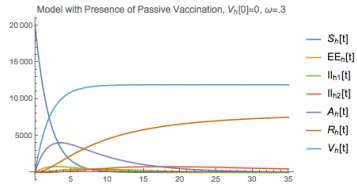

Figure 79: $\omega = .3$

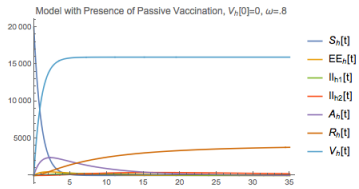

Figure 80: $\omega = .8$

As ω increases, a passive vaccination strategy grows more and more effective than a live strategy. When $\omega = .1$, a live vaccine yields only $V_{h2}[35] \approx 1900$ (Figure 41) while a passive vaccine yields $V_h[35] \approx 6700$ (Figure 78). When $\omega = .3$, we observe even greater changes, as a live vaccine yields $V_{h2}[35] \approx 3100$ (Figure 42) while a passive vaccine yields $V_h[35] \approx 12000$ (Figure 79). Likewise, in the extreme case when $\omega = .8$, a live vaccine yields $V_{h2}[35] \approx 4000$ (Figure 43) while a passive vaccine yields $V_h[35] \approx 15900$ (Figure 80) – corresponding to $\frac{4}{5}th$ of the population in the immune compartment at $t = 35$ in comparison to just $\frac{1}{5}th$ of the population under live conditions. Thus, a large-scale view elucidates that the growth of the immune compartment as ω increases is consequential for passive vaccination – at approximately 4 times the impact for live vaccination when ω is large.

Similarly, on the small scale, a change in ω plays a much greater role for passive than for active

immunization. As Figures 81 – 83 show, as ω progresses from .1 to .3 to .8, the peak of the infected population drops appreciably, especially in relation to the barely perceptible changes in Figures 44 – 46.

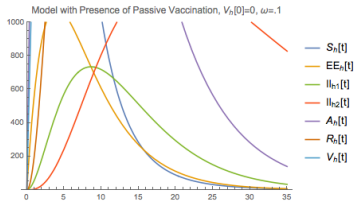

Figure 81: $\omega = .1$: A Close View.

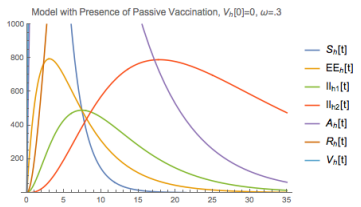

Figure 82: $\omega = .3$: A Close View.

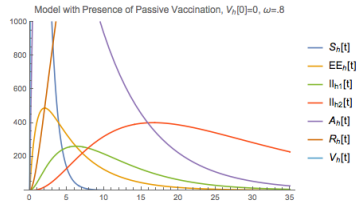

Figure 83: $\omega = .8$: A Close View.

Beginning with $\omega = .1$, a live vaccine yields $I_{h1}[10] \approx 900$ (Figure 44) while a passive vaccine yields only $I_{h1}[9] \approx 700$ (Figure 81); and when $\omega = .3$, a live vaccine yields $I_{h1}[9] \approx 880$ (Figure 45) while a passive vaccine yields $I_{h1}[8] \approx 480$ (Figure 82). And most significantly, at the extreme value of $\omega = .8$, a live vaccine yields $I_{h1}[9] \approx 810$ (Figure 46) while a passive vaccine yields $I_{h1}[7] \approx 250$ (Figure 83). Thus, choosing ω wisely can cause a much less intense outbreak with passive conditions. Additionally, the value of ω has a greater effect on the timescale of an outbreak for passive vaccination; when ω is as large as .8, in live conditions the number of days that the outbreak takes to reach peak conditions is 9; but in passive conditions, the number of days to reach the lesser peak reduces to just 7, and the outbreak runs its course more quickly. Thus, under passive conditions, such a change in ω not only causes a reduction in the amount of individuals directly impacted by ZIKV, but also a small reduction in the amount of time that the total population is affected by the outbreak.

Thus for passive vaccination, varying ω when $V_h[0] = 0$ has the potential to yield a similar impact to a preemptive vaccination strategy. However, in ideal conditions we strive for both $V_h[0] > 0$ and for the value of ω to be large. We consider the impact when $V_h[0] = \frac{N_h}{6}$ and when $V_h[0] = \frac{5N_h}{6}$. Figures 84 and 85 recall transmission dynamics when $V_h[0] = \frac{N_h}{6}$ on both the large and the small scale, with ω set to the initial estimate of .02.

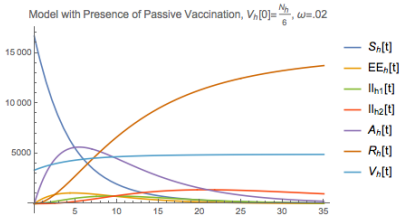

Figure 84: $\frac{1}{6}$ Human Population Immune in Advance of ZIKV Introduction, with Initial Conditions.

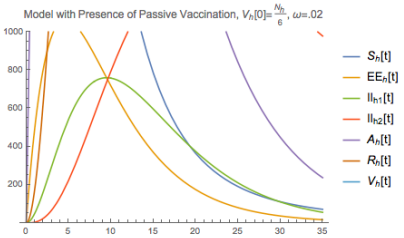

Figure 85: $\frac{1}{6}$ Human Population Immune in Advance of ZIKV Introduction, with Initial Conditions: A Close View.

If a major vaccination strategy grants passive immunity to 30% of the susceptible population per day, the corresponding rise in ω to .3 has a much larger impact than with active immunity under these conditions, too. While such a change in ω has a slight positive effect on outbreak dynamics with live vaccination – with the size of the immune compartment progressing from $V_{h2}[35] \approx 4000$ when $\omega = .02$ (Figure 53) to $V_{h2}[35] \approx 6000$ when $\omega = .3$ (Figure 55); the same change causes the size of the immune compartment to grow at a much faster rate with passive vaccination – moving from $V_h[35] \approx 4850$ when $\omega = .02$ (Figure 84) up to $V_h[35] \approx 13000$ when $\omega = .3$ (Figure 86).

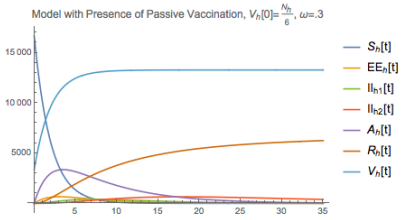

Figure 86: $\frac{1}{6}$ Human Population Immune in Advance of ZIKV Introduction, with $\omega = .3$.

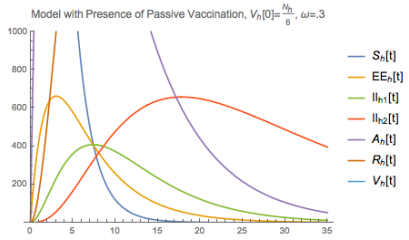

Figure 87: $\frac{1}{6}$ Human Population Immune in Advance of ZIKV Introduction, with $\omega = .3$: A Close View.

So at $t = 35$ under such conditions, a passive vaccine confers immunity to approximately 7000 more individuals than a live vaccine; thus a passive strategy protects approximately 65% of the entire population while a live strategy protects only 30%. In addition, zooming in on the small scale, a value of $\omega = .3$ under passive conditions causes I_{h1} to peak approximately 47% lower and 2 days earlier than when $\omega = .02$, with $I_{h1}[10] \approx 750$ in Figure 85 and $I_{h1}[8] \approx 400$ in Figure 87. Recalling that under live conditions this increase in ω causes I_{h1} to peak only approximately 8% lower and 1 day earlier than when $\omega = .02$, with $I_{h1}[10] \approx 800$ in Figure 54 and $I_{h1}[9] \approx 735$ in Figure 56, we recognize that varying ω yields far more consequential change for a passive vaccination campaign when $V_h[0] = \frac{N_h}{6}$.

Hence, under passive conditions a higher ω value is very important when $V_h[0]$ remains minimal.But as $V_h[0]$ grows large, we evaluate how the impact of varying ω changes. Figures 88 and 89 recall transmission dynamics on the large and small scale when $V_h[0] = \frac{5N_h}{6}$ in the presence of a passive strategy.

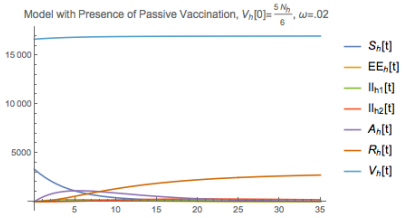

Figure 88: $\frac{5}{6}$ Human Population Immune in Advance of ZIKV Introduction, with Initial Conditions.

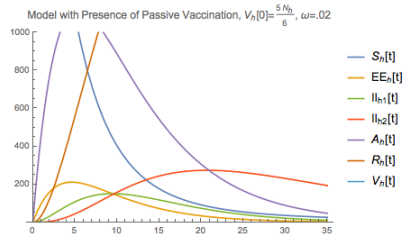

Figure 89: $\frac{5}{6}$ Human Population Immune in Advance of ZIKV Introduction, with Initial Conditions: A Close View.

When ω moves from .02 to .3 under these conditions, we record only a modest improvement in the transmission of ZIKV – similar to that of live vaccination. On the large scale, this advance in ω causes approximately an additional 9.5% of the entire population to have immunity by $t = 35$, with $V_h[35] \approx 16,900$ in Figure 88 and $V_h[35] \approx 18,800$ in Figure 90, with Figure 90 corresponding to a total of approximately 94% of the entire population with immunity.

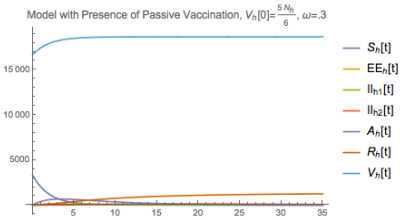

Figure 90: $\frac{5}{6}$ Human Population Immune in Advance of ZIKV Introduction, with $\omega = .3$.

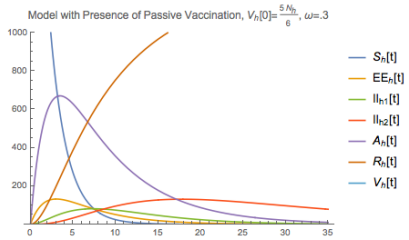

Figure 91: $\frac{5}{6}$ Human Population Immune in Advance of ZIKV Introduction, with $\omega = .3$: A Close View.

In comparison to live vaccination, we recall that by $t = 35$, $V_{h2}[35] \approx 16,750$ (Figure 59) and $V_{h2}[35] \approx 17,150$ (Figure 61) – with Figure 61 representing a total of approximately 86% of the entire population.

On the small scale, improvements in varying ω remain only minimally greater for a passive than for an active immunization strategy at this high value of $V_h[0]$. As Figure 91 depicts, a value of $\omega = .3$ causes I_{h1} to peak approximately 36% lower and 2.5 days earlier than when $\omega = .02$, with $I_{h1}[7.5] \approx 80$ compared to $I_{h1}[10] \approx 125$ (Figure 89). However, this 36% drop only demonstrates great consequence on the small scale, corresponding to only approximately .23% of the total population at this peak. Thus, like on the large scale, the effectiveness of passive conditions with such a change in ω surpass that of live conditions only slightly. Recalling that a live vaccine causes I_{h1} to peak approximately 6% lower and $\frac{1}{2}$ days earlier when ω moves from .02 to .3, with $I_{h1}[10] \approx 160$ in Figure 59 and $I_{h1}[9.5] \approx 150$ in Figure 61 – we observe that a passive vaccine minimizes the duration and intensity of an outbreak to such a small degree that differences between the types of immunization under these conditions are negligible on the large scale.

Therefore, a change in ω is still more significant for passive vaccination than for live vaccination when $V_h[0] = \frac{5N_h}{6}$ – but to a much lesser degree than when $V_h[0] = \frac{N_h}{6}$. Under these initial conditions ($V_h[0] = \frac{5N_h}{6}$), both types of vaccination strategies yield similar results at like values of ω, accentuating the previous result that the less time-sensitive passive vaccine has far greater potential for success when the initial size of the immune compartment is small. But as $V_h[0] \to N_h$, margins of change due to an increase in the passive vaccination rate grow more and more minimal, and the distinction between the effects of passive and live vaccination blurs.

In the case that the immune compartment is empty at $t = 0$ – in which a passive vaccination strategy may yield the greatest advantage over a live strategy – the passive strategy with an ω value of .42 may yield as significant of a decrease in the severity of a ZIKV outbreak as a live vaccination strategy when the immune compartment contains $\frac{2}{3}rd$ of the human population at $t = 0$. As Figures 92 and 93 demonstrate, the size of the immune compartment at $t = 35$ is approximately equal to 13250 in both cases, with $V_{h2}[35] \approx 13250$ under live conditions – shown in yellow – and $V_h[35] \approx 13250$ under passive conditions – shown in light blue.

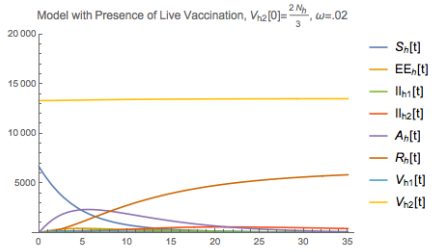

Figure 92: Model Behavior in Presence of Live Vaccine, with $\frac{2}{3}$ Human Population Immune in Advance of ZIKV Introduction, with $\omega = .02$.

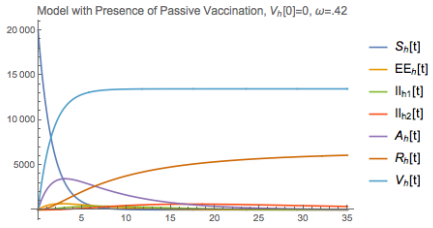

Figure 93: Model Behavior in Presence of Passive Vaccine, with None of Human Population Immune in Advance of ZIKV Introduction, with $\omega = .42$.

Thus, while preemptive vaccination is ideal and still important in combating the spread of ZIKV, a passive strategy has the potential for a *comeback* in controlling disease transmission when $t > 0$, while a live strategy does not. As these figures emphasize, with passive immunization, the same effects of early vaccination may be achieved through the realization of a large enough ω value. While incredibly high ω values may be impractical and the feasibility of $\omega = .42$ remains ambiguous, the potential impact of this value is striking in contrast to the small impact of ω under conditions of live vaccination.

Therefore, we have assessed the influence of a passive immunization strategy for managing the transmission of ZIKV, highlighting changes to $V_h[0]$ and ω. Increasing $V_h[0]$ yields significant results – drastically reducing the intensity of a ZIKV outbreak – but in comparison to live vaccination, passive vaccination

yields greater improvements in transmission dynamics when $V_h[0]$ is small; passive vaccination is effective to essentially the same degree as live vaccination when $V_h[0]$ is large. Similarly, when $V_h[0]$ is small, increasing ω shows great consequence for passive immunization in comparison to active immunization, with the change between the two types of vaccination growing smaller and smaller as $V_h[0] \to N_h$. But when $V_h[0]$ is in fact small, a passive strategy is incredibly more effective than a live strategy. Hence, time is much less important in a passive vaccination campaign – due to the immediate protection from ZIKV that such a vaccine confers. So while results improve as $V_h[0]$ grows large, the initial size of the immune compartment is much less significant, indicating that the start time of a passive vaccination campaign is remarkably less essential than that of a live vaccination campaign.

Hence, if a vaccine were not able to be administered before the start of an outbreak of ZIKV, a mass passive vaccination campaign would be a community's strongest defense in fighting the disease. Similar to live vaccination, the feasibility of this strategy depends on the practicality of a large-scale, highly accessible, and publicly supported vaccination campaign.

6.3 Protection from Mosquito Bites

Self-protection from mosquito bites to avoid contracting ZIKV can be very influential in stopping the spread of the disease. The less humans that get bit by mosquitoes, the lower the mosquito biting rate a – corresponding to less vectorial transmission of ZIKV. We recall that at $a = 0$, it is impossible for ZIKV to enter a population at all.

As Figures 94 and 95 demonstrate, when a is large, S_h drops immediately as the infectious populations $\{E_h, I_{h1}, I_{h2}\}$ spike, with transmission dynamics displaying a much more severe outbreak than with the initial parameter estimate of a, .5.

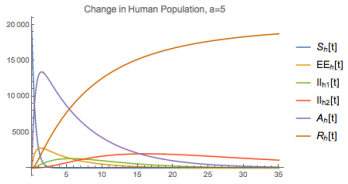

Figure 94: Large Mosquito Biting Rate Large ($a = 5$); a is set well beyond the highest value in the parameter range (1).

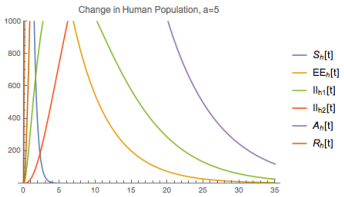

Figure 95: Large Mosquito Biting Rate: A Close View.

However, as $a \to 0$, the impact that a ZIKV outbreak has on the population diminishes greatly. Figures $96 - 98$ demonstrate large-scale changes while Figures $99 - 101$ demonstrate small-scale changes.

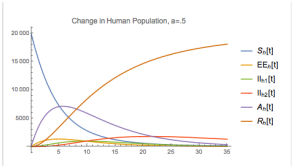

Figure 96: Average Mosquito Biting Rate ($a = .5$); a is set to the initial estimated parameter value.

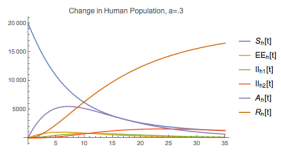

Figure 97: Low Mosquito Biting Rate ($a = .3$); a is set to the lowest value in the parameter range.

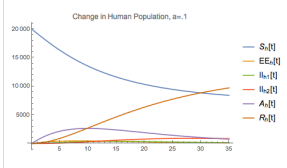

Figure 98: Very Low Mosquito Biting Rate ($a = .1$); a is reduced beyond the lowest value in the parameter range.

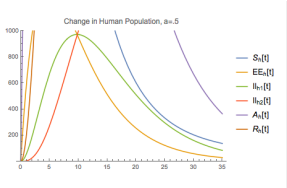

Figure 99: Average Mosquito Biting Rate.

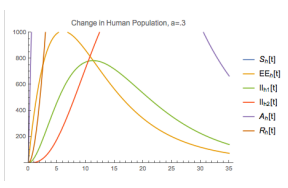

Figure 100: Low Mosquito Biting Rate.

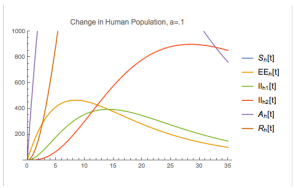

Figure 101: Very Low Mosquito Biting Rate.

These images emphasize the directly proportional relationship between a and the impact of an outbreak on the population. According to Figures $99 - 101$, as a moves from .5 to .3 to .1, the peak of the differential curve of the infected population progresses from $I_{h1}[10] \approx 960$ to $I_{h1}[12] \approx 750$ to $I_{h1}[14] \approx 400$. So reducing a yields significant results, not only in minimizing the size of the infected compartment but also in slowing down the progression of ZIKV throughout the population – causing a longer but less influential and more controllable outbreak with greater response time.

Hence, a serious strategy to prevent mosquito bites has the potential to be very successful in controlling ZIKV. However, even if susceptible humans take extreme care in wearing protective clothing and utilizing mosquito nets and repellent, the feasibility of this strategy remains unclear. It may not be possible to reduce the mosquito biting rate to a value as low as .1 – corresponding to Figures 98 and 101 – signifying that every mosquito bites a human only once every 10 days.

6.4 Control of Mosquito Populations: Reduction in Total Number of Mosquitoes m

Control of ZIKV transmission through extermination of mosquito populations, too, can be very impactful. The less mosquitoes that exist, the less vectors that may carry the disease – corresponding to a lower average ratio of mosquitoes to humans m, in range $[1, 10]$. Logically, if mosquito populations are completely eradicated and thus $m = 0$, then it is impossible for ZIKV to have any effect on an entirely susceptible human population. As Figure 102 demonstrates, the disease simply does not transmit if there are no mosquitoes to transmit it.

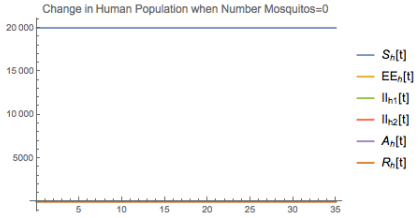

Figure 102: Model Behavior with No Mosquitoes in System ($m = 0$). This demonstrates a disease-free state of the population.

But when m is large, the influence of a ZIKV outbreak is intensified, with a larger number of vectors to infect additional humans. When $m = 10$ – the highest value in the parameter range – transmission dynamics with the initial parameter estimate $m = 5$ are exemplified. In comparison to these base case conditions shown in Figures 105 and 108, Figures 103 and 104 display that for $m = 10$, S_h diminishes at a faster rate, as the disease spreads throughout the population more quickly, impacting its entirety by $t = 23$ – as opposed to t beyond the range of $[0, 35]$ when $m = 5$. The close-up view elucidates that the peak of the size of the infected population has a higher value and occurs more quickly for $m = 10$ than $m = 5$, too; Figure 104 indicates that $I_{h1}[8] \approx 1100$ while Figure 108 indicates that $I_{h1}[10] \approx 960$.

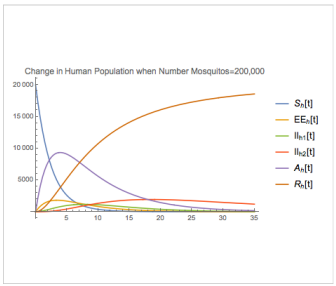

Figure 103: Average Ratio of Mosquitoes to Humans $10:1$ ($m = 10$).

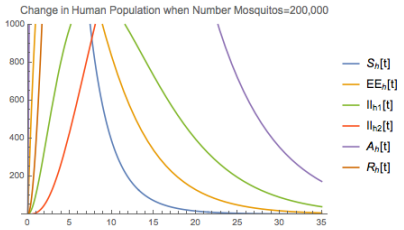

Figure 104: Average Ratio of Mosquitoes to Humans $10:1$: A Close View.

Yet as $m \to 0$, the severity of a ZIKV outbreak shrinks immensely, with a striking decrease in transmission of the disease observed once the total number of mosquitoes becomes equal to the total number of humans in the system ($m = 1$). This relationship between m and outbreak intensity is similar to that of a and outbreak intensity, but the impact of varying m is significantly more effectual. Figures $105 - 107$ demonstrate large-scale changes while Figures $108 - 110$ demonstrate small-scale changes.

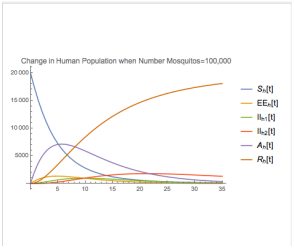

Figure 105: Average Ratio of Mosquitoes to Humans $5:1$ ($m = 5$).

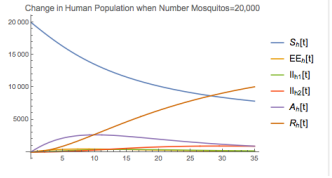

Figure 106: Average Ratio of Mosquitoes to Humans $1:1$ ($m = 1$).

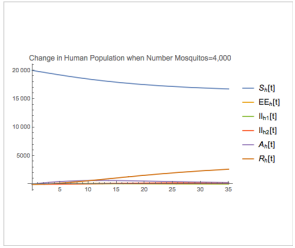

Figure 107: Average Ratio of Mosquitoes to Humans $.2:1$ ($m = .2$).

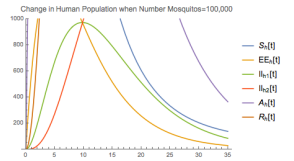

Figure 108: $m = 5$.

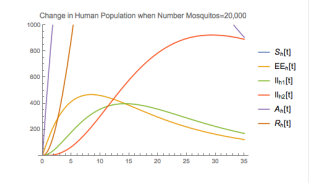

Figure 109: $m = 1$.

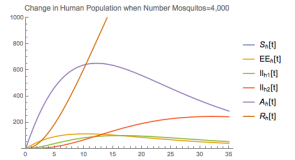

Figure 110: $m = .2$.

Hence, like a, the relationship between m and the influence of a ZIKV outbreak is directly proportional. As m progresses from 5 – the base case – to 1 – the lowest value in the parameter range – to .2 – beyond this minimum – the proportion of the total human population that is impacted by the disease drastically decreases. As Figures $108 - 110$ reflect, the peak of the differential curve of the infected population progresses from $I_{h1}[10] \approx 960$ to $I_{h1}[15] \approx 400$ to $I_{h1}[16] \approx 100$. As m grows small, the development of the outbreak not only slows down, but also corresponds to a momentous change in the size of the infected population, declining to only 10.4% of its initial size at peak time.

Therefore, a committed strategy to eradicate mosquito populations has the capacity to be extremely successful in managing the spread of ZIKV. However, like extreme protection from mosquito bites, the practicably of this strategy is uncertain. While Figures 107 and 110 demonstrate vastly improved conditions, it may not be realistic to deplete the mosquito population to such an extent that there is only 1 mosquito per every 5 humans ($m = .2$). Further, even if this strategy were viable, it may be cost-prohibitive or environmentally destructive to take such extreme action in reducing mosquito populations.

6.5 Limiting Sexual Transmission of ZIKV

While controlling sexual transmission of ZIKV is important in that safe sex obstructs vertical transmission of the disease and thus reduces the incidence of microcephaly and other complications related to pregnancy, it does not have a significant impact on outbreak dynamics. We recall that changing the sexual transmission rate β – even drastically – has a very minimal effect on the rates of change of the human populations. A smaller β does correspond to a decline in the severity of a ZIKV outbreak, but to such a small degree that the impact is barely perceptible.

Figures 111 and 112 portray transmission dynamics when $\beta = 0$, depicting conditions when vectorial transmission is the only mode of passing on the virus.

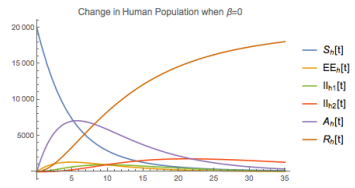

Figure 111: No Sexual Transmission Rate ($\beta = 0$).

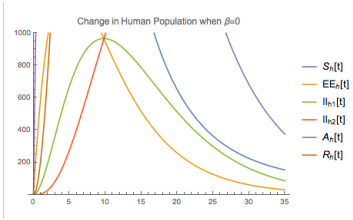

Figure 112: No Sexual Transmission Rate: A Close View.

Yet, as β grows large, the influence of a ZIKV outbreak on the total population shows essentially no change. Figures $113 - 115$ elucidate that on the large-scale, changes are negligible. As β moves from .05 to .1 to 1, transmission dynamics are nearly identical to the β-free state of Figure 111. The estimated range for this parameter is $[.001, .1]$, so $\beta = 1$ is well beyond the realistic confines of this variable. But even with this impossibly high value, the only noticeable change in the system is that S_h drops at a slightly faster rate.

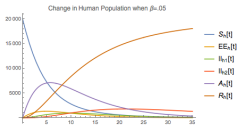

Figure 113: Average Sexual Transmission Rate ($\beta = .05$); β is set to the initial estimated parameter value.

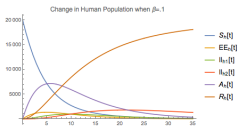

Figure 114: High Sexual Transmission Rate ($\beta = .1$); β is set to the highest value in the parameter range.

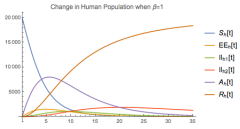

Figure 115: Extremely High Sexual Transmission Rate ($\beta = 1$); β is set unrealistically far beyond the highest value in the parameter range.

Even zooming in to range $[1, 1000]$ indicates minimal change. Figures $116 - 118$ demonstrate the progression of human population dynamics on this small scale. As β increases, the peak of the differential curve of the infected population progresses from $I_{h1}[10] \approx 970$ to $I_{h1}[10] \approx 975$ to $I_{h1}[10] \approx 1050$, in comparison to $I_{h1}[10] \approx 965$ when $\beta = 0$ (See Figure 112). Thus, focusing closely on this range demonstrates conspicuous change only when β is unrealistically large, and even at $\beta = 1$, changes remain modest.

Figure 116: Average Sexual Transmission Rate.

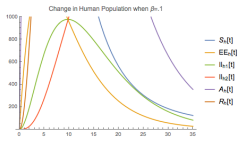

Figure 117: High Sexual Transmission Rate.

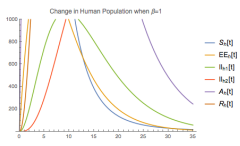

Figure 118: Extremely High Sexual Transmission Rate.

Hence, these figures emphasize that while in ideal conditions β will be as low as possible, the relationship between β and the spread of ZIKV throughout a population is trivial. While promoting safe sexual contact

and comprehensive accessibility to contraception remain important, adjusting β does not have the capacity to stop or even appreciably slow an outbreak of ZIKV. Therefore, other strategies must be the focal point of controlling the spread of the virus.

7 Conclusion

Based on these results, the best strategic response to the Zika virus is a mass live vaccination campaign – if instituted before $t = 0$. Because of the long-lasting effect of a live vaccine, this strategy is preferable to a passive vaccine if immunizations begin before ZIKV begins to impact a population. In this case, the vaccine has time to become effective and confer active immunity upon the community before individuals are ever exposed to the virus. For live vaccination, immunization must be preemptive. However, if the virus has already been introduced into the population, a passive vaccination campaign is recommended, due to the immediacy of passive immunity. Such a strategy may effectively combat disease transmission when $t > 0$, while a live strategy may not.

While both self-protection from mosquito bites and community control of mosquito populations enact positive change in preventing the spread of ZIKV, and taking measures to mitigate sexual transmission of the virus remains important, an immunization strategy persists as the most pragmatic way to combat the Zika virus on a large scale. Thus, it is crucial to prioritize the completion of a successful Zika vaccine in order to achieve global protection from ZIKV.

8 Acknowledgments

Throughout this project, my thesis advisor, Dr. Andrea Bruder, has been a crucial source of support and encouragement. I would like to express my gratitude for her ongoing guidance and for sharing her expertise in epidemiological modeling and numerical simulations, specifically in Mathematica. I would also like to thank my professors Dr. Damiano Fulghesu and Dr. David Brown for inspiring my interest in differential modeling throughout my ordinary and partial differential equation courses. Additionally, I would like to thank the Department of Mathematics and Computer Science at Colorado College for supporting my growth as a student throughout my undergraduate studies.

References

[1] Atkinson B, Hearn P, Afrough B, Lumley S, Carter D, Aarons EJ, et al (2016) Detection of Zika Virus in Semen. Emerging Infectious Diseases 22(5):940. https://dx.doi.org/10.3201/eid2205.160107

[2] Barrett ADT (2018) Current status of Zika vaccine development: Zika vaccines advance into clinical evaluation. NPJ Vaccines 3(24). https://doi.org/10.1038/s41541-018-0061-9

[3] Brauer F, Castillo-Chavez C (2012) Epidemic Models. In: Antman S, Institute for Physical Science and Technology (ed) Mathematical Models in Population Biology Epidemiology, 2nd edn. Springer, New York, pp 345-409

[4] Edelstein-Keshet, L (2005). Applications of Continuous Models to Population Dynamics: The Population Biology of Infectious Diseases. In: O'Malley R (ed) Mathematical Models in Biology, SIAM edn. Society for Industrial and Applied Mathematics, Philadelphia, pp 242-256

[5] Foy BD, Kobylinski KC, Foy JL, Blitvich BJ, Travassos da Rosa A, Haddow AD, et al (2011) Probable Non–Vector-borne Transmission of Zika Virus, Colorado, USA. Emerging Infectious Diseases 17(5):880-882. https://dx.doi.org/10.3201/eid1705.101939

[6] Hills SL, Russell K, Hennessey M, et al (2016) Transmission of Zika Virus Through Sexual Contact with Travelers to Areas of Ongoing Transmission — Continental United States, 2016. Morbidity and Mortality Weekly Report 65:215–216. http://dx.doi.org/10.15585/mmwr.mm6508e2

[7] Gao D, Lou Y, He D, Porco T, Kuang Y, Chowell G, Ruan S (2016) Prevention and Control of Zika as a Mosquito-Borne and Sexually Transmitted Disease: A Mathematical Modeling Analysis. Scientific Reports 6. https://doi.org/10.1038/srep28070

[8] Gourinat A, O'Connor O, Calvez E, Goarant C, Dupont-Rouzeyrol M (2015) Detection of Zika Virus in Urine. Emerging Infectious Diseases 21(1):84-86. https://dx.doi.org/10.3201/eid2101.140894

[9] The history of Zika virus. World Health Organization. https://www.who.int/emergencies/zika-virus/timeline/en/

[10] Immunity Types. Centers for Disease Control and Prevention: Vaccines and Immunizations. https://www.cdc.gov/vaccines/vac-gen/immunity-types.htm. Accessed 10 February 2020

[11] Kucharski A, Funk S, Eggo R, Mallet H-P, Edmunds W, Nilles E (2016) Transmission Dynamics of Zika Virus in Island Populations: A Modelling Analysis of the 2013–14 French Polynesia Outbreak. PLoS Neglected Tropical Diseases 10(5). https://doi.org/10.1371/journal.pntd.0004726

[12] Massad E, Coutinho FAB, Wilder-Smith A (2019) Modelling an optimum vaccination strategy against ZIKA virus for outbreak use. Epidemioly & Infection 147:e196. https://doi.org/10.1017/S0950268819000712

[13] Shah N, Patel Z, Yeolekar B (2017) Preventions and Controls on Congenital Transmissions of Zika: Mathematical Analysis. Applied Mathematics 8:500-519. https://doi.org/10.4236/am.2017.84040

[14] Usman, S, Isa Adamu, I, Babando, H (2017) Mathematical Model for the Transmission Dynamics of Zika Virus Infection with Combined Vaccination and Treatment Interventions. Journal of Applied Mathematics and Physics 5:1964-1978. https://doi.org/10.4236/jamp.2017.510166

[15] Vaccines. Victoria State Government: Better Health Channel. https://www.betterhealth.vic.gov.au/health/healthyliving/vaccines/. Accessed 4 February 2020

[16] (2019) Zika Epidemiology Update. World Health Organization. https://www.who.int/emergencies/diseases/zika/epidemiology-update/en/. Accessed 21 January 2020

[17] (2016) Zika situation report. World Health Organization. https://www.who.int/emergencies/zika-virus/situation-report/4-august-2016/en/

[18] Zika Virus Vaccines. National Institute of Allergy and Infectious Diseases. https://www.niaid.nih.gov/diseases-conditions/zika-vaccines. Accessed 21 January 2020

[19] (2018) Zika Virus. World Health Organization. https://www.who.int/news-room/fact-sheets/detail/zika-virus. Accessed 11 October 2019

[20] (2017) WHO/UNICEF Zika Virus (ZIKV) Vaccine Target Product Profile (TPP): Vaccine to protect against congenital Zika syndrome for use during an emergency. World Health Organization, UNICEF. https://www.who.int/immunization/research/development/WHO_UNICEF_Zikavac_TPP_Feb2017.pdf?ua=1. Accessed 21 January 2020